



## Scholars' Mine

---

[Doctoral Dissertations](#)

[Student Theses and Dissertations](#)

---

1970

# Higher space mode analysis of a large cylindrical pulsed H<sub>2</sub>O system

Harold David Hollis

Follow this and additional works at: [https://scholarsmine.mst.edu/doctoral\\_dissertations](https://scholarsmine.mst.edu/doctoral_dissertations)

 Part of the [Nuclear Engineering Commons](#)

**Department: Mining and Nuclear Engineering**

---

### Recommended Citation

Hollis, Harold David, "Higher space mode analysis of a large cylindrical pulsed H<sub>2</sub>O system" (1970). *Doctoral Dissertations*. 2046.  
[https://scholarsmine.mst.edu/doctoral\\_dissertations/2046](https://scholarsmine.mst.edu/doctoral_dissertations/2046)

This thesis is brought to you by Scholars' Mine, a service of the Missouri S&T Library and Learning Resources. This work is protected by U. S. Copyright Law. Unauthorized use including reproduction for redistribution requires the permission of the copyright holder. For more information, please contact [scholarsmine@mst.edu](mailto:scholarsmine@mst.edu).

HIGHER SPACE MODE ANALYSIS  
OF A LARGE CYLINDRICAL PULSED H<sub>2</sub>O SYSTEM

by

HAROLD DAVID HOLLIS, 1932-

A DISSERTATION

Presented to the Faculty of the Graduate School of the

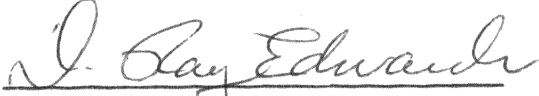
UNIVERSITY OF MISSOURI-ROLLA


DOCTOR OF PHILOSOPHY

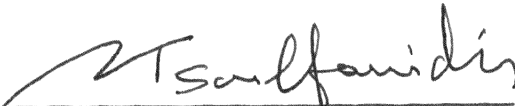
in

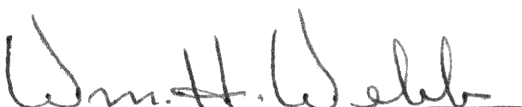
NUCLEAR ENGINEERING

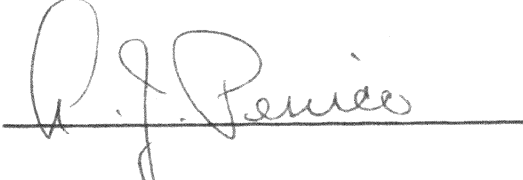
1970

  
\_\_\_\_\_  
Advisor

  
\_\_\_\_\_

  
\_\_\_\_\_

  
\_\_\_\_\_

  
\_\_\_\_\_

## ABSTRACT

By utilizing a geometrically centered pulsed source internal to a large ( $B_g^2 \approx 0.002$ ) cylindrical  $H_2O$  system, the neutron flux was measured as a function of position and time. A least square fit of the data yielded the fundamental and five higher decay constants and amplitudes of the thermal neutron flux. Symmetrical and enhanced neutron densities were obtained as a result of the internal source. Long waiting times were unnecessary and data acquisition was accelerated.

The decay constants were found to be independent of position, pulse width, counting time and rates, method of normalization, or waiting time. The decay constants were related to the bucklings by an analysis of the amplitudes without variance of the size of the system.

This method gives  $\Sigma_a v = (4759 \pm 54) \text{ sec}^{-1}$ ,  $D_0 = (3.7084 \pm 0.0897) \times 10^4 \text{ cm}^2/\text{sec}$ ,  $L = (2.79 \pm 0.05) \text{ cm}$ ,  $\sigma_a^H = (323 \pm 3) \text{ mb}$ , and a mean neutron lifetime of  $(210 \pm 2.4) \mu\text{sec}$ .

## ACKNOWLEDGMENTS

The first and foremost expression of appreciation should go, in this case, to the author's wife, Barbara. Her patience, understanding, and assistance has prevailed through many years. Her fortitude should not go unrewarded and to this end, the author would like to dedicate this work to her.

Special thanks should go to Dr. D. R. Edwards, who as advisor and friend, has assisted and guided this work to a successful conclusion. Thanks should go also to Dr. A. E. Bolon, Dr. A. J. Penico, Dr. H. Kim, Dr. N. Tsoulfanidis, and especially Dr. W. H. Webb for their kindness and help as members of the author's committee. Dr. W. H. Webb initially encouraged the author to enter the field and has been instrumental in obtaining educational funding.

Without the assistance of Mr. Dan Poole, of the reactor staff, this work would have been just that, work. Thanks should be expressed for the callouses, both physical and mental, developed during the assembly, construction, and modification of the apparatus and associated components and shielding. His operation of the generator over long hours, lunch periods, and after his working day is appreciated. Thanks to Mr. Murv Little, also of the reactor staff, the electronics remained operational, however obstinate. His ability to "kiss" and coax the components was invaluable.

The author would like to thank the Computer Science Department of the University and in particular the operators of the computer, Tom DeWald, Lynn Carter, Charles Irwin, and James Williams, as well

as Mike Martin and David Dearth. This experiment could never have been accomplished without the analysis by a computer.

Acknowledgment should be made to the Division of Nuclear Education and Training of the United States Atomic Energy Commission for the equipment and also for the indirect funding of a traineeship and three Oak Ridge Atomic Energy Special Fellowships. This financial support enabled the author to pursue the most worthwhile goals of knowledge and educational productivity.

None of the people listed above are responsible or accountable for errors of commission or omission perpetrated herein.

## TABLE OF CONTENTS

|  | Page |
|--|------|
| ABSTRACT . . . . .                             | ii   |
| ACKNOWLEDGMENTS . . . . .                      | iii  |
| LIST OF ILLUSTRATIONS . . . . .                | vi   |
| LIST OF TABLES . . . . .                       | viii |
| I. INTRODUCTION . . . . .                      | 1    |
| II. APPARATUS . . . . .                        | 6    |
| A. GENERATOR AND TANK . . . . .                | 6    |
| B. DATA ACQUISITION SYSTEM . . . . .           | 10   |
| III. EXPERIMENTAL PROCEDURES . . . . .         | 16   |
| A. PREPARATIONAL PROCEDURES . . . . .          | 16   |
| B. OPERATIONAL PROCEDURES . . . . .            | 18   |
| IV. DATA ANALYSIS . . . . .                    | 22   |
| V. DESCRIPTION OF DATA ANALYSIS . . . . .      | 27   |
| VI. SOURCE EFFECTS AND NORMALIZATION . . . . . | 32   |
| VII. RESULTS AND CONCLUSIONS . . . . .         | 33   |
| A. GENERAL RESULTS AND CONCLUSIONS . . . . .   | 33   |
| B. LABORATORY APPLICATION . . . . .            | 41   |
| BIBLIOGRAPHY . . . . .                         | 42   |
| VITA . . . . .                                 | 44   |
| APPENDICES . . . . .                           | 45   |
| I. STATISTICS . . . . .                        | 45   |
| II. RECOMMENDATIONS . . . . .                  | 51   |
| III. BUCKLINGS AND AMPLITUDES . . . . .        | 54   |

## LIST OF ILLUSTRATIONS

| Figure   | Page |
|--|------|
| 1. Schematic Cross Section of Generator and Tank . . . . .                           | 7    |
| 2. Schematic Diagram of System and Shielding . . . . .                               | 8    |
| 3. Detection and Storage System . . . . .  | 11   |
| 4. Pulse of Generator. . . . .   | 13   |
| 5. Output of Preamplifier. . . . .   | 13   |
| 6. Output of Amplifier . . . . .   | 14   |
| 7. Output of Preamplifier. . . . .   | 14   |
| 8. Analyzer Data . . . . .   | 15   |
| 9. Analyzer Data . . . . .   | 15   |
| 10. Anomalous Decay Curve . . . . .  | 19   |
| 11. Decay Constants Versus Buckling . . . . .  | 39   |
| 12. Decay Constants Versus Buckling . . . . .  | 40   |
| 13. Total Relative Amplitude Versus Axial Position. . . . .                          | 58   |
| 14. Total Relative Amplitude Versus Radial Position . . . . .                        | 59   |
| 15. Relative Amplitude Versus Axial Distance for I=1. . . . .                        | 60   |
| 16. Relative Amplitude Versus Axial Distance For I=3. . . . .                        | 61   |
| 17. Relative Amplitude Versus Axial Distance For I=5. . . . .                        | 62   |
| 18. Relative Amplitude Versus Axial Distance For I=13 . . . . .                      | 63   |
| 19. Relative Amplitude Versus Radial Distance For J=1 . . . . .                      | 64   |
| 20. Relative Amplitude Versus Radial Distance For<br>Higher Modes With J=1 . . . . . | 65   |

## LIST OF ILLUSTRATIONS (cond.)

| Figure   | Page |
|--|------|
| 21. Relative Amplitude Versus Radial Distance For $J=2$ . . . .                                | 66   |
| 22. Relative Amplitude Versus Distance Along $45^\circ$<br>Direction For $I=1, J=1$ . . . . .  | 67   |
| 23. Relative Amplitude Versus Distance Along $45^\circ$<br>Direction For $I=5, J=1$ . . . . .  | 68   |
| 24. Relative Amplitude Versus Distance Along $45^\circ$<br>Direction For $I=13, J=1$ . . . . . | 69   |



## LIST OF TABLES

| Table                                    | Page |
|--|------|
| I. DESCRIPTION OF DATA SETS . . . . .    | 23   |
| II. DIFFUSION PARAMETER RESULTS. . . . . | 34   |
| III. ANALYSIS RESULTS . . . . .          | 35   |
| IV. CALCULATIONAL RESULTS. . . . .       | 36   |
| V. STATISTICAL RESULTS. . . . .          | 46   |
| VI. STATISTICAL RESULTS. . . . .         | 47   |
| VII. CORRECTED DATA SET . . . . .        | 50   |

## I. INTRODUCTION

There has been a plethora of literature on and about pulsed neutron techniques and applications during the last decade. Review articles (1,2,3,4,10,19,25,26) are numerous and well cover the state of the art, results, and advances achieved. This work is an addition to this body of description and is intended as a basic coordination of fundamental ideas. No thermalizing medium is required as a result of the source being located directly in the medium being investigated. In addition, the symmetrically located source does not require a large amount of shielding and produces a symmetric neutron density. Higher modes were utilized to obtain the diffusion parameters rather than volume or geometrical changes. This eliminated the necessity of waiting until the higher modes decayed away and the consequent loss of information or counting statistics. The counting acquisition time and total number of counts in time was increased.

The common technique utilized is to create a short source or burst of fast neutrons either outside or at the boundary of the medium to be investigated. (2,26) By using a thermalizing medium or waiting a sufficient length of time, the asymptotic fundamental decay of the thermal neutron density may be investigated. (2) In the present work, the source was located centrally in the medium being investigated and the lowest six of the decay modes were considered.

Initially the fast neutrons lose energy through scattering for a period called the slowing down time. The second phase of moderation, called thermalization is where the neutrons lose energy until a state

of thermal equilibrium is attained with the moderating medium. In this state, a space distribution is achieved, asymptotic in time and energy.

To describe the neutron population with a differential equation, one turns to the Boltzmann equation in the diffusion approximation for an isotropic, bare, homogeneous medium for thermal energies.

$$-D(E)\nabla^2\Psi(E,\bar{r},t) + \Sigma_a(E)\Psi(E,\bar{r},t) = -\frac{1}{V} \frac{\partial \Psi(E,\bar{r},t)}{\partial t} \quad [1]$$

Since sufficient time has elapsed from the initial pulse, there is no source term for the downscatter or input of fast neutrons. Assuming that the thermal flux is space and energy separable, one then can express:

$$\Psi(E,\bar{r},t) = \psi(E)N(\bar{r},t) \quad [2]$$

and further that

$$N(\bar{r},t) = \sum_{lm} A_{lm}(\bar{r})e^{-\lambda_{lm}t} \quad [3]$$

Equations[1] to [3] are valid under the following assumptions:

1. The flux is finite over all space and time.
2. The axial and radial first derivatives of the flux at the axial and radial centerlines are zero.
3. Sufficient time has elapsed to establish a thermal flux (13).
4. The diffusion approximation is valid.
5. The thermal lifetime is long compared to thermalization time.
6. The flux vanishes at the extrapolated boundaries.

Three and five are good assumptions for large hydrogenous systems. One, two, and six were verified experimentally, and four is valid where boundaries and sources are excluded or avoided.

The expressions [2,3] yield

$$\lambda_{1m} = \lambda_0 + D_0 B_{1m}^2 \quad [4]$$

where the buckling  $B_{1m}^2$  is obtained from

$$\nabla^2 \Psi_{1m}(\bar{r}) + B_{1m}^2 \Psi_{1m}(\bar{r}) = 0 \quad [5]$$

yielding

$$B_{1m}^2 = (l\pi/H)^2 + (\alpha_m/R)^2 \quad [6]$$

The amplitude term has been expressed as a form of

$$A_{1m} \cos \frac{l\pi z}{H} J_0(\alpha_m \frac{r}{R}) \quad (23)$$

where

$\lambda_0 = \Sigma_a v$  or infinite decay constant

$D_0 =$  diffusion coefficient  $= vD$

$H =$  extrapolated height

$R =$  extrapolated radius

$\alpha_m =$  root of the zero-order Bessel function,  $J_0$

$l = 1, 3, 5, \dots$

$m = 1, 2, 3, \dots$

The diffusion cooling from [4] and all subsequent terms may be eliminated due to the small value of the buckling in the present work. During the period of thermal diffusion, the energy spectrum and the thermal space distribution are considered constant with a time decrease in amplitude. This investigation considered the higher harmonics present in the thermal flux following the burst of fast neutrons and after the die-away of the source and epi-cadmium contributions.

Equation 4 gives the  $\lambda_0$  or  $v\Sigma_a$  as the zero buckling intercept,  $D_0$  or diffusion coefficient as the slope at zero, and  $C_0$ , the

diffusion cooling from the least squares fitting of the  $\lambda$  vs.  $B^2$  curve. The diffusion length is obtained by the distance along the  $B^2$  axis at the extrapolated ( $\lambda = 0$ ) point. The present work considers the various bucklings inherent in the higher modes. The resultant decay constants of averages of many spatial points were plotted with respect to the associated bucklings. Various recipes are employed using the various decay constants to obtain the diverse time relationships of thermalization of the system considered. These will be given utilizing the present obtained decay values.

The "waiting" times recommended (11) to eliminate higher harmonics were disregarded in this work as was an associated thermalizing medium, i.e., the medium employed to thermalize the source neutrons prior to entering the medium being investigated. The "waiting time" for conventional experiments would be of the order of milliseconds or larger while in this work, the waiting time was of the order of a few hundreds of microseconds.

Least square fitting of the data was utilized to obtain amplitudes and decay constants. Eight terms were considered. The amplitudes were found to be comparable in magnitude for six decay constants, which is in opposition to current considerations (7). As a direct result of the "elimination" of waiting time, the total count rate for a given period of time is enhanced considerably. Further enhancement of the data is achieved by being able to consider data with good ratios of peak channel to background counts even for a much shorter data acquisition time.

Higher modes were obtained in both radial and axial directions (7) in contrast to previous work (11). This method of higher mode analysis appears to be more precise being tedious only in the time required for computer analysis. The six decay constants were found to be independent of pulse width, repetition rate, number of points, number of harmonics, or the position of the detector. The internal neutron source improved the count rate and the fundamental decay mode may be determined simply in elementary laboratories by this method without complications of data acquisition time, changes in the system, or elaborate electronic systems.

The inherent disadvantages of small systems and/or large thermalizing systems have been eliminated in this work. The fitting of the data was by least squares analysis rather than Fourier analysis; reasonable and rather agreeable results have ensued. The centrally located source produces a symmetric neutron density that facilitates analysis.

## II. APPARATUS

The equipment used in this experiment may be broken down into two categories; the generator with tank and the data acquisition system. These will be described in the following sections.

### A. GENERATOR AND TANK

The generator was a model A-1250 positive ion accelerator by Kaman Nuclear (9). This unit could produce a neutron yield of  $2.5 \times 10^{11}$  neutrons/second in continuous mode. The drift tube assembly was such (68 cm) that the target could be located in the center of the tank assembly. The generator was mounted on a dolly enabling the operators to adjust the height to position the tank receiver tube or to remove the drift tube and target assembly from the tank for repairs or inspection.

A sheet metal "track" was built to guide the generator system in and out of the shielding well and receiver tube. This restricted the dolly motion so that the target would be positioned correctly in the tank and to eliminate damage to the drift tube and target assembly. A movable motor driven shielding cart was designed and built to mobilize the shielding directly behind the generator to facilitate maintenance and access to the generator. Layouts of these devices appear in figures 1 and 2.

The pulse width and repetition rate of the generator and multi-channel analyzer was regulated at the console of the generator. The pulse which triggered the generator also started the time sequenced mode of the multichannel analyzer. The pulse rate and duration were

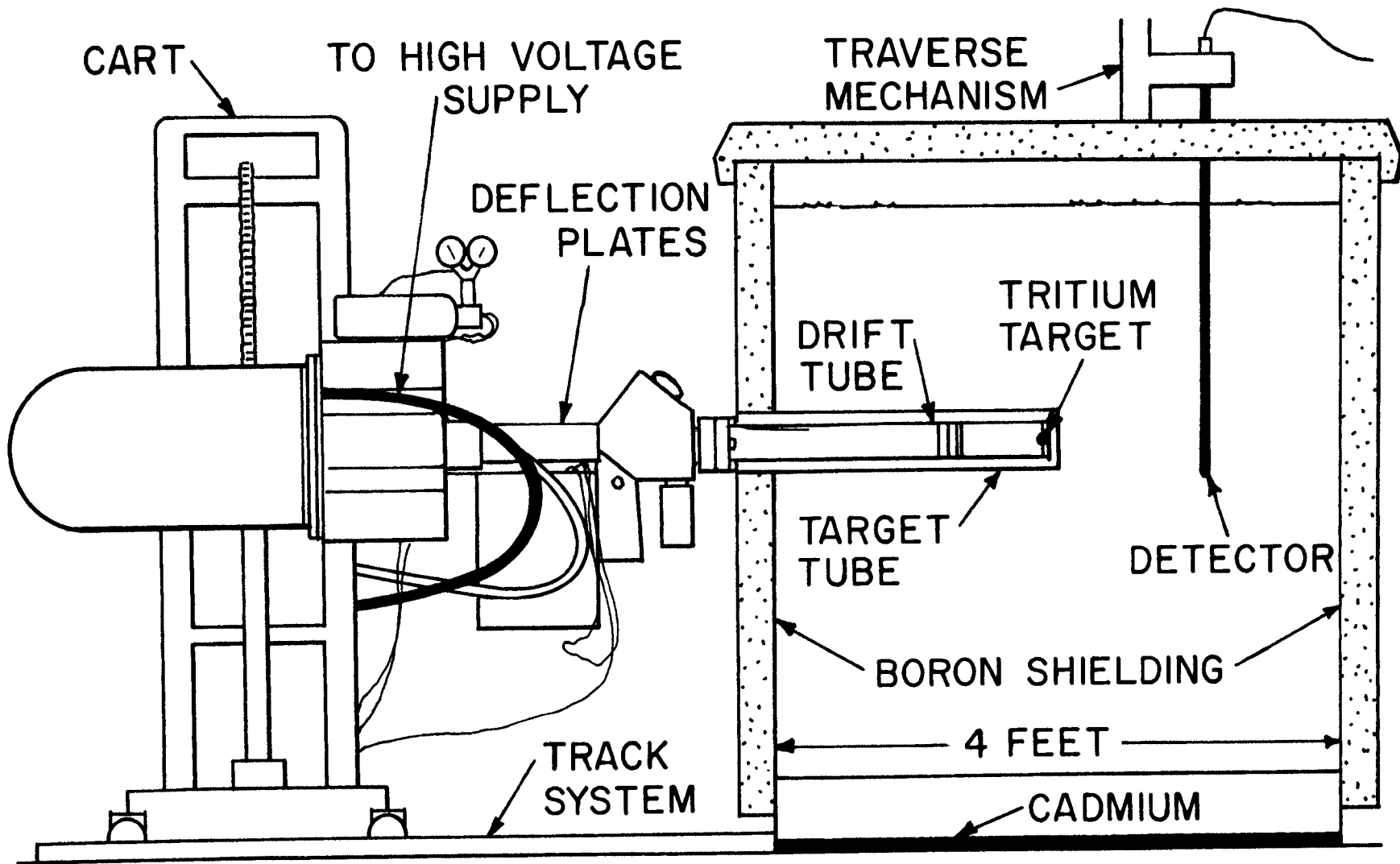


FIGURE 1. SCHEMATIC CROSS SECTION OF GENERATOR AND TANK



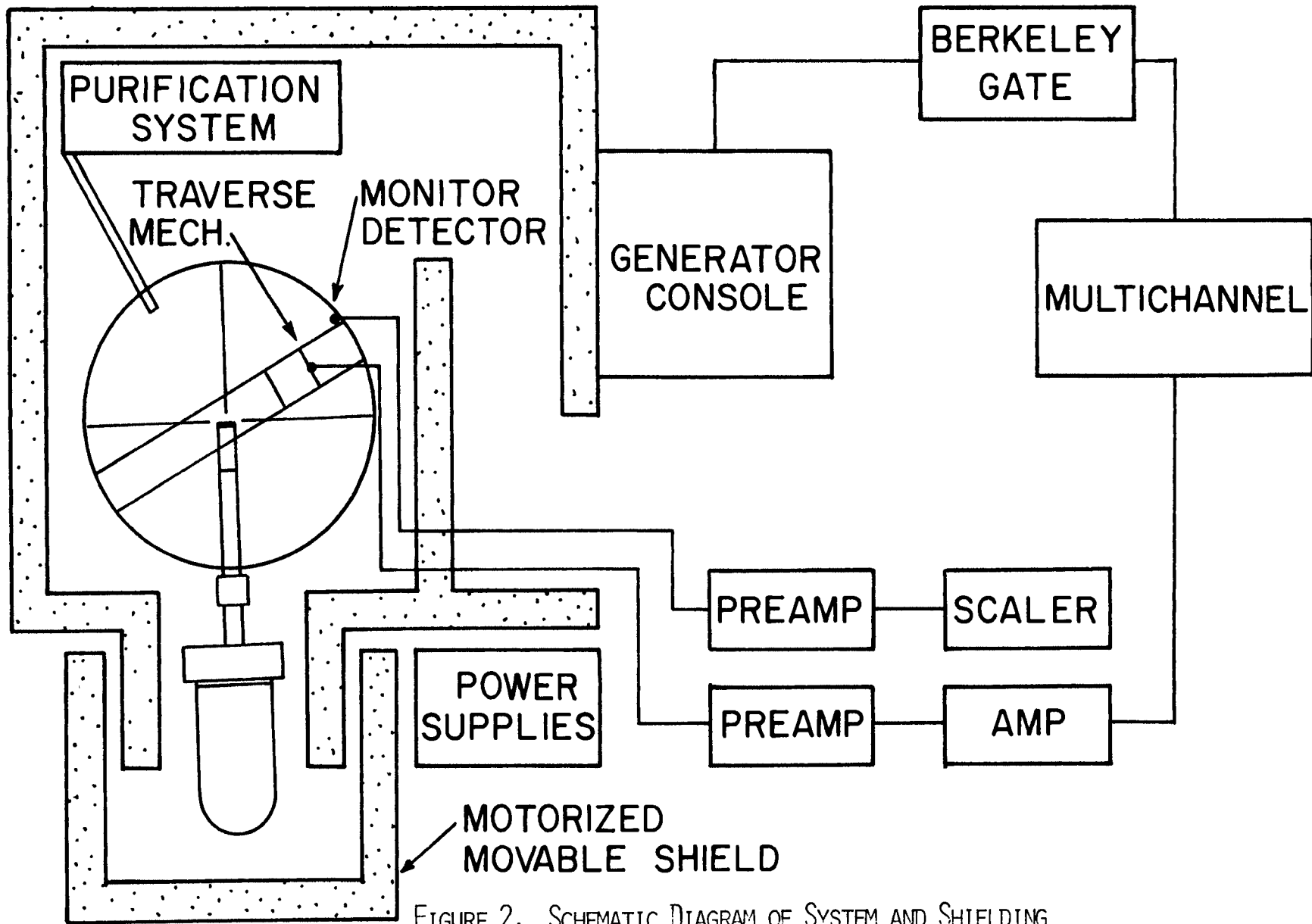


FIGURE 2. SCHEMATIC DIAGRAM OF SYSTEM AND SHIELDING

varied to check results. While pulsing with a duty cycle around 1 per cent, the beam current was less than 10  $\mu$ amp time averaged.

Figure 4 is an oscilloscope trace of the "pulse" of the generator as seen by the operator. This was obtained (6) by viewing the target current by an oscilloscope. The die away of the pulse during all operations regardless of the pulse width remained less than 20 $\mu$  seconds.

Figure 1 gives a schematic cross section of the generator and tank. The tank is almost a right circular cylinder ( $R = 24$  in.,  $H_{\text{water}} \cong 50$  in.). The tank receiver tube for the drift tube and target assembly were constructed at the UMR Technical Services shop as was the detector traverse mechanism. The traverse mechanism allowed accurate locations of the detector with respect to the center of the tank. It could be operated manually or by use of an electric drive mechanism either horizontally or vertically.

The traverse or positioning mechanism (figure 2) could be manually moved in any particular radial direction and due to the optimal motion imparted to the detector, was invaluable in the collection of data along a  $45^\circ$  line.

The tank was surrounded by a two inch thick layer of boric acid. The boric acid was placed in commercial plastic bags which were packed around the tank and were held in position by aluminum sheets strapped around the tank. It was observed empirically that the thermal flux directly outside this shielding during generator operation was the same as the background when the generator was off, thus creating a zero boundary.

The tank was filled with water from the UMR reactor pool. The water was mechanically filtered and continuously run through an ion filter indigenous to the system tank. This water was periodically cycled into the reactor filter system and replaced from the reactor pool to maintain purity. The constancy of the water temperature ( $22.40 \pm .05$  C<sup>o</sup>) was probably due to the volume of the system, location in the reactor bay area, and the proximity of tons of shielding.

#### B. DATA ACQUISITION SYSTEM

Figure 3 is a block schematic of the detection and storage system used. Starting with the detector, through to but not including the analyzer, there is a twin system set up but only one side was used for data acquisition.

The detector was selected to minimize active and overall volume and the need for a long length. It was a proportional BF<sub>3</sub> thermal neutron detector with a one inch active length, sensitive volume of 1 cm<sup>3</sup>, and a diameter of 5/16 inch (Reuter-Stokes RSN-1055). The detector positions were sufficiently far from the source to preclude significant radiation damage effects from the source. The two pre-amplifiers were Hewlett-Packard 5554A's. These pre-amplifiers have a time constant of one microsecond and were found to be excellent operational devices. The signal was then amplified by an ORTEC 485 amplifier. The input to the analyzer is thus separated by selective voltage amplification and the utilization of the analyzer threshold (-10 volts) as a discriminator.

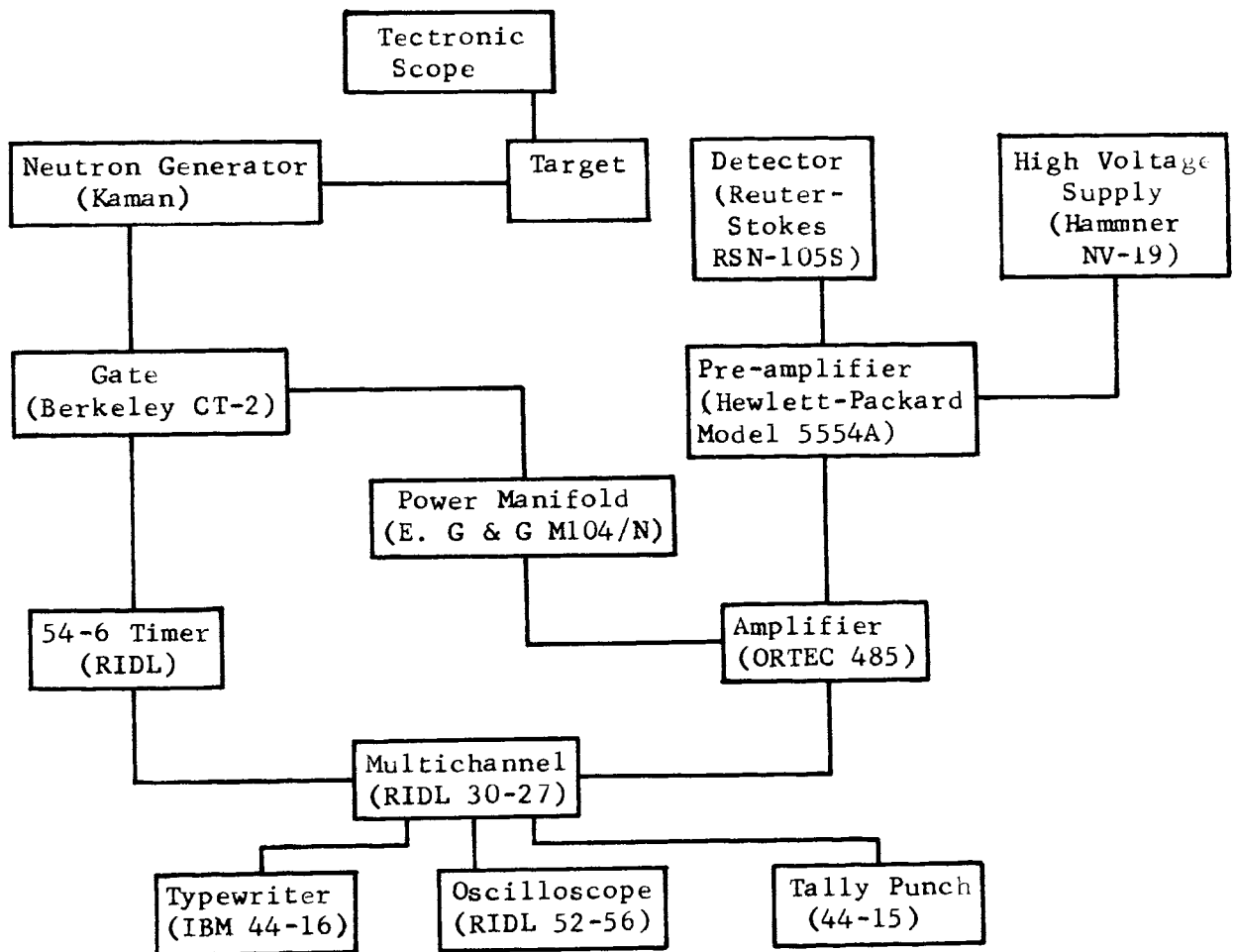


FIGURE 3. DETECTION AND STORAGE SYSTEM

The multichannel analyzer was a RIDL 34-27 series Scientific Analyzer system with a model 24-2 400 word memory. The analyzer was operated in the time sequenced mode (multi scaler operation). This arrangement of the analyzer gave a maximum count capacity of  $(10^5 - 1)$  with a maximum pulse repetition rate of one megacycle. The system responded to pulses with a resolution time of one microsecond. A model 54-6 time base generator was used to control channel dwell and start the analyzer upon reception of the trigger pulse from the console of the generator via the Gate Generator (Berkeley, BNC) Model CT-2. The switching time between channels was 12.5 microseconds with the system being able to count one count during this interval.

In addition, the data being stored or previously stored could be inspected by use of a RIDL Model 52-56 display oscilloscope. The data was output either on an IBM model 44-15 typewriter or on a Tally model 44-15 tape punch, or as was the usual case, both.

Figures 4, 5, 6, 7, 8, and 9 are oscilloscope traces of the outputs of the various devices listed previously.

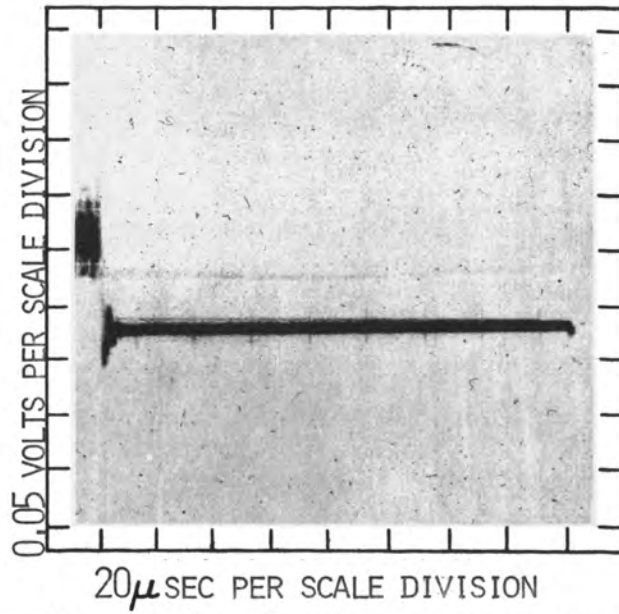


FIGURE 4: PULSE OF GENERATOR

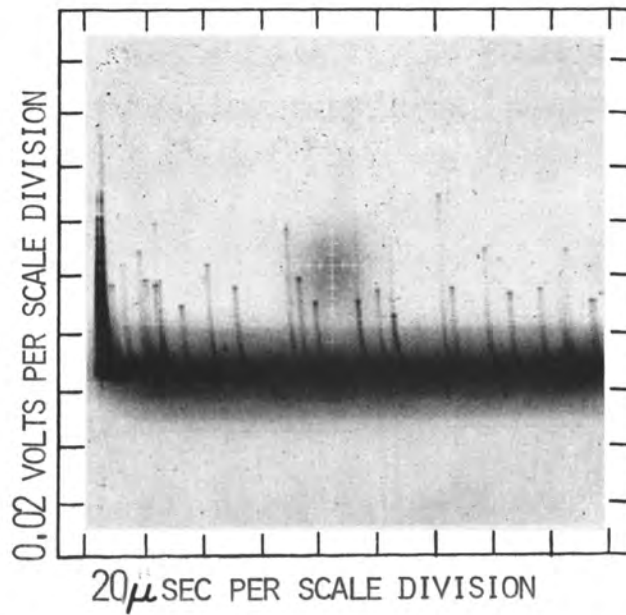


FIGURE 5: OUTPUT OF PREAMPLIFIER

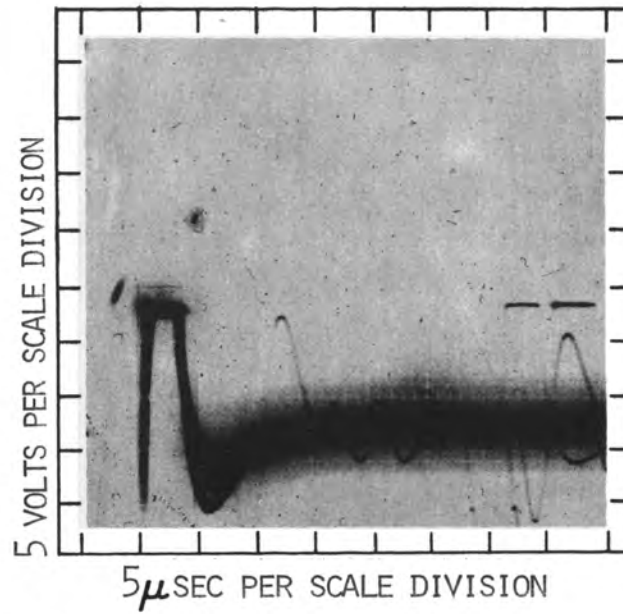


FIGURE 6: OUTPUT OF AMPLIFIER

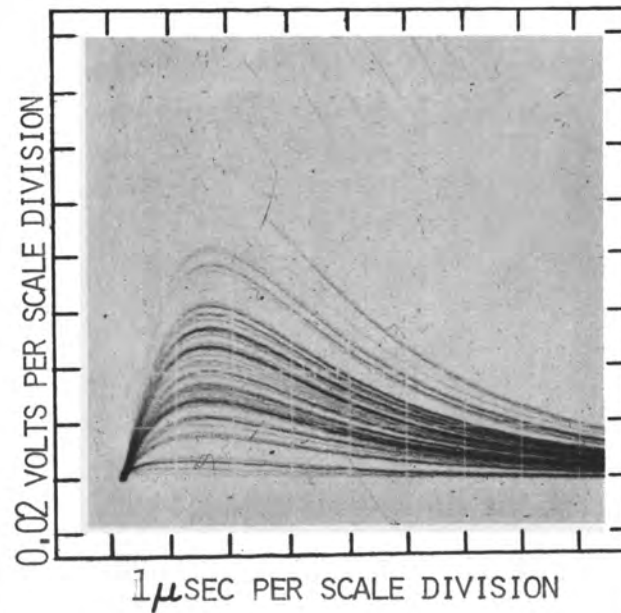
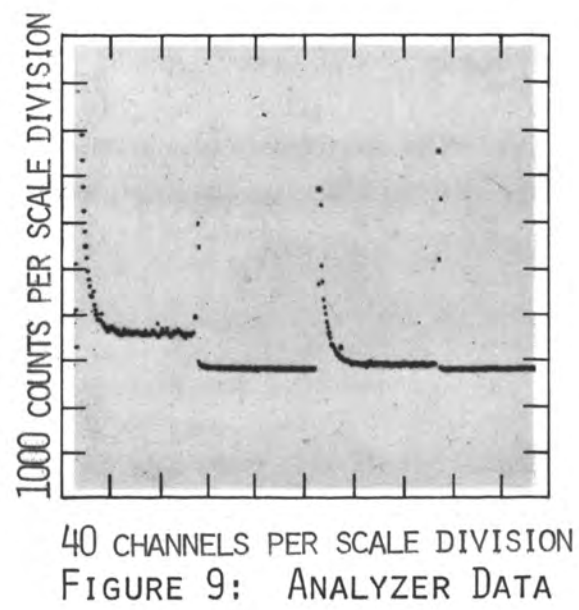
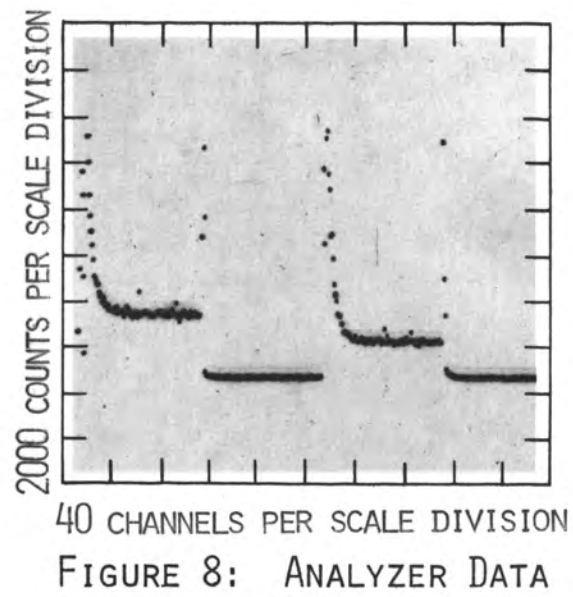


FIGURE 7: OUTPUT OF PREAMPLIFIER





### III. EXPERIMENTAL PROCEDURES

#### A. PREPARATIONAL PROCEDURES

The characteristic operational voltage of the flux probe detector was periodically checked utilizing the entire system. The multichannel dwell time was set and by periodically advancing the voltage, the characteristic detector curve could be displayed on the analyzer oscilloscope in segment form. A Pu-Be neutron source was used to check the plateau of the neutron counter as well as the channel-wise response of the multichannel analyzer. The operational plateau did not change during the entire time of data acquisition. The trigger pulse was utilized, with the neutron generator off, to start the multichannel and check the input to each channel. The system was allowed to count the constant source for long periods of time to assure uniform deposition of pulses in each channel.

An amplification check was periodically performed to assure a minimum amplification necessary to eliminate noise and background with the Pu-Be source removed and sufficient counts with the source present. Problems of spurious electrical pulses affecting isolated channels in the analyzer were encountered. These channel "jumps" were eliminated from the data and an averaged value of the adjacent channels was substituted before the data was analyzed. Apparently there are stray fast voltage changes in the supply voltage to the analyzer that are random. In addition, changing scale during data acquisition introduces jumps. No data run was utilized with over two spurious channels and only six of these were acceptable; that is,

the jump was sufficiently large to demonstrate that it was spurious.

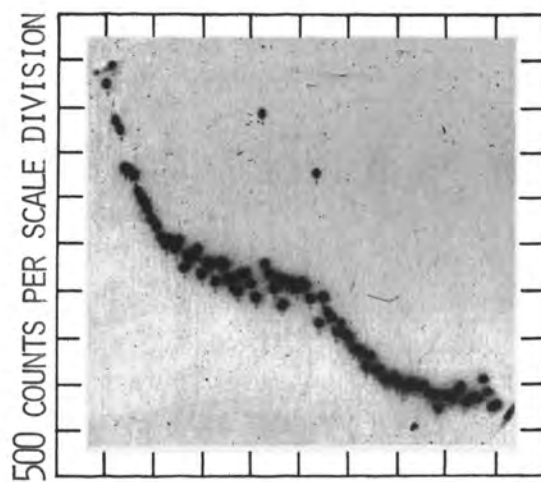
The water temperature did not vary appreciably over the period of the measurement. This was determined by checking regularly. The purity remained between 3 to 5 megohms centimeter. With each set of data taken, such as a sweep across the tank, a normalization run was taken close to the source to assure a fairly uniform output of the generator for a given time duration of count. This was in addition to the observable output of the generator at the console and on the oscilloscope just as a check against the magnitude of the output both during the bare run and the cadmium cover run. This also allowed a magnitude check of the peak to background ratio.

During initial trial runs, the pulse width was varied from 3 microseconds to fifty microseconds. A pulse width of 35 to 50 microseconds gave satisfactory counting statistics for the counting times used and at any distance from the source. Runs were consequently made at both widths. At pulse widths of from 3 to 6 microseconds, two "peaks" were observed. These could more properly be called two distinct decays. Initially, the detecting, storing, or generator system was suspect, however, these hopes were dashed when the detector position was varied and the peaks were found to be dependent on position. Close to the source, the first peak was predominant and the second was not observed. At large distances from the source, the first decay was "gone" and the second shape was left. The two decay shapes appeared visually to have very strikingly similar shapes. The frequency of pulsing was varied to determine that overlap was not

occurring. Channel dwell time was varied but this duality persisted. Another detector, another system (utilization of the analog system of the analyzer), checks on the off time of the generator were performed and tried, however, with negative results of elimination. In an abortive attempt to credit this phenomena to rate dependence of the detection system, a pulse generator was substituted for the detector and with operational settings the same, the system was found to be rate independent to 40,000 cts/sec. The flux range of the detector is 10 to  $10^6$  n/cm<sup>2</sup>-sec. With up to fifty microsecond pulse width, the counting statistics did not reach these levels in channels used for decay analysis. After these investigations, it was found that a pulse width of thirty-five to fifty microseconds not only gave better counts at large distances but also "overdrove" the existence of the two decays. Figure 10 is an oscilloscope photo of the counts in the multichannel on a 5 K scale with a detector distance of 5 inches. This was a 15 minute run at 14 cyc/sec. with a pulse width of 3.5  $\mu$ sec. and a total generator trace pulse die-away of < 20  $\mu$ sec.

#### B. OPERATIONAL PROCEDURES

Twenty minute runs were selected since this gave a ratio of corrected peak channel to background ratio of from 100 to about 30 depending on the relative position of the detector from the source ( $10^4$  uncorrected). 25 cycles per second pulse repetition rate was arbitrarily chosen to allow die out of the background and to maximize the counts obtained. Thus 0.0375 seconds elapsed between end of count



10 CHANNELS PER SCALE DIVISION

FIGURE 10: ANOMALOUS DECAY CURVE

and the initiation of a new pulse. The multichannel dwell time was 12.5 microseconds with 12.5 microseconds between channels, giving 0.0025 total count time for 100 channels. One hundred channels were used for a bare detector run and the next hundred were used for a cadmium covered detector run. This process was followed for the last two hundred channels of the 400 and then the data stored was output. Two hundred channels could have been used for each run; however, no additional information would be obtained. 35 and 50 microsecond pulse width runs were taken so as to compare amplitudes. The gate was set for no delay and the gate start pulse width was set arbitrarily to 10 microseconds.

The detector locations were chosen arbitrarily to obtain a fair representation of the amplitude map across the core and no attempt was made to reduce the effects of any harmonics. A few mean free paths distance was maintained for separation between the detector and both the source and boundaries when points were chosen close to either. Otherwise, there was no discrimination on selection of position of the detector. All sweeps, except one, were made from the source out to the boundary. The detector would be positioned, a bare 20 minute run would be made. Then the cadmium cover would be placed over the detector and the epi-cadmium 20 minute run would be completed; then the cadmium cover would be removed and the detector would be repositioned for the next run.

There was sufficient time lapse between sweeps of the target by the deuterium beam to allow one of the principal causes of background

to die out. This is the time varying portion due to creation of neutrons by the generator during the off target time and by room return of fast and intermediate neutrons. The other principal background is the steady state, which is relatively constant. Both backgrounds were relatively small with respect to the channel contents and were treated as a constant. The epi-cadmium measurements were subtracted from the total counts thus effectively eliminating the epi-cadmium room return to the detector.

To avoid possible end-effects near the water-air interface at the top of the tank, data points were not taken close to the surface. Furthermore, the possibility of room returns near the top of the tank appeared small. This was checked by locating the detector near the top of the tank. A 200 channel run did not display any unexpected variations for long periods of counting. The channel contents dropped to the steady state background relatively quickly with no channels past 13 containing appreciable counts above statistical background.

## IV. DATA ANALYSIS

For the various runs, the detector was placed at a given position in the system and a decay curve was obtained both for a bare detector run and a cadmium covered run. Table I lists the various group runs.

The background encountered was relative to the position of the detector; however, since the raw data taken were relative also, it did not adversely affect the results. Figures 8 and 9 are oscilloscope photos of typical sets of data accumulated in the multichannel. The counts in the background channels, the last 50 channels of the data sequence, decreased as the detector was moved away from the source. The raw data count was thus shifted down in magnitude as the detector position from the source was increased as may be seen in figures 8 and 9. These were data sets at distances of 5, 7, 9, 11 inches respectively. Each four hundred channels covers two data sets. After being output and converted onto computer cards, the raw data were then adjusted by normalizing for those runs where the amplitude of the output of the generator was not relatively equivalent. The raw data were then "dead time" corrected by the relation

$$C = \frac{C_J'}{1 - T C_J'}$$

where  $C_J'$  = count rate recorded

T = deadtime of  $BF_3$  counter

In this work, the response dead time was 1  $\mu$ sec, the channel width was 12.5  $\mu$ seconds, and the overall effect of this factor was rate independent over the utilized range of channels except for

TABLE I  
DISCRIPTION OF DATA SETS

| <u>Direction</u>        | <u>Detector Positions</u>                  | <u>Pulse Widths</u>              |
|-------------------------|--|----------------------------------|
| radial                  | 90° to left of source<br>tube--same plane  | 50 μsec.                         |
| radial                  | 90° to right of source<br>tube--same plane | 50 μsec.                         |
| radial                  | 180° from source tube--<br>same plane      | 35 μsec<br>(for reproducibility) |
| radial                  | 180° from source tube--<br>same plane      | 50 μsec                          |
| axial                   |  | 50 μsec                          |
| axial                   |  | 35 μsec<br>(for reproducibility) |
| 45° radial<br>and axial | 180° from source tube                      | 50 μsec                          |
| 45° radial<br>and axial | 180° from source tube                      | 50 μsec<br>(for reproducibility) |



positions very near the source.

The counts obtained with the cadmium covered detector were subtracted from the counts obtained with the bare detector to obtain the "corrected" thermal counts. Channels 50 to 100 (the last half of the corrected thermal sequence channels) were then averaged to obtain a background and then subtracted.

The resultant counts in the first 100 sequence were then utilized in the Los Alamos Least Squares Program (12,15) to obtain the decay constants and amplitudes. This program is a non-linear least square fit of a function  $y = f(X_i, \alpha_i)$  where the  $n$  observations of  $y$  are the dependent variables and the  $x$ 's are the independent ones.

The program minimizes

$$Q = \sum_{i=1}^N W_i [Y_i - f(X_{1i} \dots X_{mi}; \alpha_1 \dots \alpha_p)]^2$$

The weights  $W_i$  used in this case were  $1/Y_i^{1/2}$  and one. This program has been utilized (7,14) for die-away decay analysis of the form

$$Y = \sum_{j=1}^K A_j e^{-\lambda_j T}$$

The end channel of the sequence was arbitrarily required to have zero counts with the first channel used selected by the contamination of the harmonics present in the analysis. Initial computer runs started in the eighth to the thirteenth channel. With subsequent runs it was found that the "contamination" of the highest amplitudes and decay constants (nonsensical results) could be eliminated by moving out in time, i.e. (starting in the thirteenth channel) increasing the starting channel number. The amplitudes and decay

constants "contaminated" are characterized by very large decay constants and arbitrary amplitudes. As the starting time is increased, these decay constants get smaller and the amplitudes "firm up". The first six decay constants were readily apparent no matter what starting channel was used. The seventh was found by this method and the eighth was neglected due to the large amount of computer time required to converge the large number of points on a large decay constant. The results on the seventh and eighth will be given, although the confidence is small. Most data sets consisted of several decades of channels and very large amounts of computer time was utilized (over 100 hours).

The program was allowed to iterate for 96 iterations and then the "trends" were accelerated and the data submitted again with the "improved" guesses. If an amplitude or decay constant changed appreciably, then there might be a corresponding fluctuation in one or more of the other parameters, during initial runs. During final runs, an intentional fluctuation would be corrected by the program.

Initially sixteen terms were chosen, i.e.

$$Y = \sum_{i=1}^{16} A_i e^{-\lambda_i T}$$

However, this number was reduced to six by combining two or more terms with similar  $\lambda_i$ 's. This was found to be erroneous and two more terms were re-introduced later. With less than six terms, the program ceased to iterate. The equation became, using the average values of the decay constants:

$$\begin{aligned}
y(\rho, T) = & A_1 e^{-297345T} + A_2(\rho) e^{-15087T} + A_{13,1}(\rho) e^{-8689T} \\
& + A_{5,1}(\rho) e^{-5436T} + A_{3,2}(\rho) e^{-5300T} + A_{1,2}(\rho) e^{-5078T} \\
& + A_{3,1}(\rho) e^{-5055T} + A_{1,1}(\rho) e^{-4834T}
\end{aligned}$$

Initial guesses were made by plotting the data and extracting calculated guesses of amplitudes and decay constants.

As was previously mentioned, there were some channels with spurious counts. These channels were averaged by taking the channels on each side. Figure 10 displays this channel "jump" by the obvious channels that definitely do not "fit" the curve. At the conclusion of data acquisition, it was found, while photographing the oscilloscope traces, that counts could be added in a channel by changing the scale while acquiring data. It was fortuitous that the operators and experimenter were not in the habit of changing the scale.

The counts in the peak channels varied around  $5 \times 10^4$  to  $10^5$  according to position and counts in channel 100 were around  $10^2$  to  $10^1$ . Counts in the cadmium covered runs varied from  $10^4$  in the peak channel to usually  $10^1$  in the last channel. Counts in the channels used for harmonic analysis were in the  $10^3$  to  $10^4$  range for the first channels to zero to 15 in the last channels used.

## V. DESCRIPTION OF DATA ANALYSIS

Initially, hand plots of data sets yielded guesses for decay constants and amplitudes. These were then utilized in the Least Squares (12,15) program and iterations began. The multiple mode phase of the data is the most difficult to analyze by hand; however, almost any reasonable value will suffice provided a small amplitude is used. None of the parameters were fixed during initial computer runs and it was empirically found that convergence is accelerated if no restrictions are placed on either the amplitudes or decay constants. In fact, if amplitudes or decay constants are fixed until convergence or test criteria is reached and then the parameters are allowed to vary, significant changes in value may be observed. As a result of these findings, all values obtained were found by not restricting the program or any parameters. A data set was considered as converged if after a large number of iterations, no change was observed in all the numbers after the first digit of the decay constants. A small value for the test criteria enabled the program to iterate down to small magnitude changes.

The starting channel was selected entirely on an economic and time basis. The two higher modes were the only parameters affected by the starting channel or the weight. Channel thirteen (325  $\mu$ sec.) was finally adopted as the starting channel since the largest mode was greatly affected by the starting channel and the next highest mode appeared to be only slightly affected. This was found by changing the starting channel after convergence of a data set and observing

the parameter changes after convergence occurred again. The weight factor  $(1/y^{1/2})$  was selected so as to give as small a relative weight difference related to the magnitude of the counts. This factor was selected; however, the values of the two highest decay constants were the only ones significantly affected when a different value was used.

The largest decay constant found ( $297345 \text{ sec}^{-1}$ ) was not only a function of starting channel but also of position. As the starting channel decreased, the magnitude also decreased. In addition, as the distance from the source is increased, the validity of this value decreases because of the weight factor and the relative decrease in counts in the first few channels for constant magnitude or time data acquisition runs.

The next highest decay mode was not a direct function of position; however, the associated amplitude was as expected. The relative dispersion of values found was sufficiently large to preclude any confidence in the values. The amplitudes became negligible as the distance from the source increased. As a result, it was impossible to assign indices identifying the decay mode and buckling. The value obtained for the slope would require very large indices associated with the buckling.

During initial computer runs, a number of decay constants appeared similar and were eliminated by summing amplitudes. It was found later that some of those eliminated were necessary for proper amplitude identification. The order of modes converging was consistently found to have decay constants of  $2.9 \times 10^5$ , 15087, 8689, 4834, 5436, and always

last was a value around 5200. Amplitude identification of this value indicated an index of one in the axial direction, a two in the radial plane, and a 3,2 in the  $45^\circ$  direction. Two values eliminated during initial computer runs were around 5100 to 5340. Two additional decay terms were inserted into the program with values of 5200 and the three resulting values were consequently found of 5078, 5300, and 5055.

Upon insertion of the two extra terms, the other amplitudes and decay constants did not change. The amplitude of the 5200 decay constant broke down and "divided" into the amplitudes of the other inserted terms. Convergence was relatively quick and the variance and other statistical parameters of the data sets so changed were improved. Not all data sets were changed since the other amplitudes and decay constants were not affected.

A comment should be made on the consistence and persistence of the 8689 decay constant during computer analysis. Intentional perturbations of the input value were corrected more quickly by the program for this decay mode than for any other parameter. Perturbing the highest decay mode was not corrected by the computer program and as a consequence of this and other indications mentioned, there is no validity to the value of the highest.

The obtained amplitudes were plotted and compared to theoretical amplitudes (2,3,22) to obtain one index in the axial direction, the second in the radial plane, and the  $45^\circ$  results were used for verification.

The computer output gave the last iteration value every 96 iterations. These values were compared to the input values and trends were

asserted. A value would be increased or decreased according to the value shown and the change in magnitude. The data sets converged from the outside positions inward with the points close to the source converging last. Some data sets were run as many as two hundred times. The axial data sets were run first and as data acquisition continued, these values of amplitudes and decay constants were input to the radial and  $45^\circ$  data sets as initial values or guesses. All parameters were free and not fixed to allow the program to change signs or magnitudes as necessary. As a consequence of the above, the changes in amplitude for a given position changed drastically for different directions. This assisted in reducing foreknowledge or bias on the part of the programmer.

Final values of the decay constants were then averaged over all data sets. The distributions were statistically analyzed for the average  $\frac{\sum \lambda_i}{N}$ , median  $\frac{\lambda_N}{2}$ , root mean square  $\sqrt{\frac{\sum (\lambda_i)^2}{N}}$ , standard deviation  $\sqrt{\frac{\sum (\lambda_i - \lambda_{ave})^2}{N-1}}$ , variance  $\frac{\sum (\lambda_i - \lambda_{ave})^2}{N-1}$ , sum of the deviations  $\sum (\lambda_i - \lambda_{ave})$ , and the mean deviation  $\frac{\sum (\lambda_i - \lambda_{ave})}{N-1}$ . The average values of the decay constants were then utilized to obtain the desired parameters.

The amplitudes of various runs for a given direction set were normalized to obtain equivalent magnitudes. Averages were then taken for a given position for the multiple runs of a given position. These steps were performed for the amplitudes of each decay constant for the

for the axial, radial, and  $45^\circ$  direction. The values obtained were then normalized to the largest value and plotted to obtain maximum and minimum values and for the distances where the sign of the amplitude changed. These plots were then compared to theoretical plots to obtain the index numbers of the respective decay constants. The computer code appeared to be not as sensitive as could be desired for the amplitudes. Perturbations of the decay constants would be quickly corrected; however, amplitude changes were not always consistent.



## VI. SOURCE EFFECTS AND NORMALIZATION

Test runs were made for a given location of the detector with parameter changes of the source. It was found as a result, that the shape in time of the data was constant; however, the amplitude changed.

This may be demonstrated also for various detector positions by comparing the oscilloscope photos of different data sets (figures 8, 9). The shapes remained constant; however the amplitude and background varied as a result of position and source intensity. By using channels 50 to 100 of a 100 channel run to average background, the necessity of maintaining accurate normalization relations was reduced.

The background, as well as the amplitude, was a function of the distance from the source. A measure of the background was also a measure of the amplitude. When the background was subtracted, the amplitudes were to some degree corrected for source variations. It was assumed that the detectors were point detectors and did not perturb the system. The runs made with a normalization detector and scaler reinforced these conclusions by the time change in data acquisition and the subsequent changes in the background for a given count. The amplitudes were very similar after background corrections. The tail of the die-away exists after 50 channels and a portion of this is included in the background. The only loss of information would be with respect to the fundamental mode; however, since it is the most persistent and smallest, this loss is negligible. There were no large discrepancies between or among runs that were normalized by either total data acquisition time or total counts in a normalizing scaler system.

## VII. RESULTS AND CONCLUSIONS

### A. GENERAL RESULTS AND CONCLUSIONS

The diffusion parameters obtained by this method are listed in Table II along with a few pertinent values from other works. The differences between measured and calculated parameters are so frequent and diverse in articles and books that a comprehensive listing would be confusing and unnecessary. The second and third works listed (11,17) also considered higher harmonics. The higher modes were not considered in these works to obtain diffusion parameters. Fourier analysis was utilized and the source was located outside the medium. Comparison values listed were very similar, the present work obtained a slightly improved value of the diffusion length  $L$ . The fourth is given as a earlier work and as a reference for buckling size. All errors listed were derived assuming maximum error possibilities.

Tables III and IV give a compendium of the values found and calculated in obtaining the diffusion parameters. The largest percentage errors are associated with the slope value  $D_0$ . The maximum high and maximum low values given were obtained by considering that the errors were cumulative and that the maximum deviations were occurring simultaneously to give the greatest possible errors. The minimum high and low values given considered more feasible standard deviation errors. The error and % error values were obtained utilizing the maximum calculations. The errors established are probably maximized beyond probability however being conservatively taken. The decay periods

TABLE II

## DIFFUSION PARAMETER RESULTS

| Method | Geometry    | Buckling<br>Tange $\text{cm}^{-2}$ | $\Sigma_a V$<br>$\text{sec}^{-1}$ | $D_0$<br>$10^4 \text{ cm}^2/\text{sec}$ | L<br>cm         | $\sigma_a^H$ (mb) | Neutron Mean<br>Lifetime $\mu\text{sec}$ | Reference               |
|--------|-------------|------------------------------------|-----------------------------------|---|-----------------|-------------------|--|-------------------------|
| Pulsed | Cylindrical | 0.002 to 0.1                       | 4759 $\pm$ 54                     | 3.7084 $\pm$ 0.897                      | 2.79 $\pm$ 0.05 | 323 $\pm$ 3       | 210 $\pm$ 2.4                            | Present Work            |
| Pulsed | Slab        | 0.014 to 0.59                      | 4768 $\pm$ 24                     | 3.7503 $\pm$ 0.366                      | 2.83 $\pm$ 0.02 | 325 $\pm$ 2       | 210 $\pm$ 1                              | (11) Lopez<br>& Beyster |
| Pulsed | Sphere      | 0.0796 to 0.37                     | 4767 $\pm$ 68                     | 3.8570 $\pm$ 0.736                      | 2.86 $\pm$ 0.03 | 323 $\pm$ 4.7     | -----                                    | (17) Nasser<br>& Murphy |
| Pulsed | Slab        | 0.006 to 0.018                     | ----                              | 3.8500 $\pm$ 0.800                      | 2.85 $\pm$ 0.05 | 328 $\pm$ 8.0     | 213 $\pm$ 4                              | (21) Scott et al        |

TABLE III  
ANALYSIS RESULTS

| Quantity         | Value     | Maximum<br>High Value | Minimum<br>High Value | Maximum<br>Low Value | Minimum<br>Low Value | Error           | % Error | Units                         |
|------------------|-----------|-----------------------|-----------------------|----------------------|----------------------|-----------------|---------|-------------------------------|
| $\lambda_{1,1}$  | 4834.391  | 4900.39               | 4863.30               | 4768.39              | 4805.48              | $\pm 66.0$      | 1.37    | $\text{sec}^{-1}$             |
| $B^2_{1,1}$      | 0.0023548 | 0.002395              |                       | 0.002315             |                      | $\pm 0.00004$   | 1.71    | $\text{cm}^{-2}$              |
| $\lambda_{3,1}$  | 5055.117  | 5126.12               | 5063.17               | 4984.12              | 5047.07              | $\pm 71.0$      | 1.41    | $\text{sec}^{-1}$             |
| $B^2_{3,1}$      | 0.0072932 | 0.0074126             |                       | 0.0071766            |                      | $\pm 0.0001194$ | 1.65    | $\text{cm}^{-2}$              |
| $\lambda_{1,2}$  | 5078.363  | 5149.36               | 5082.70               | 5007.36              | 5074.02              | $\pm 71.0$      | 1.40    | $\text{sec}^{-1}$             |
| $B^2_{1,2}$      | 0.009772  | 0.009943              |                       | 0.0096057            |                      | $\pm 0.000171$  | 1.74    | $\text{cm}^{-2}$              |
| $\lambda_{3,2}$  | 5300.004  | 5373.00               | 5308.77               | 5227.00              | 5291.23              | $\pm 73.0$      | 1.38    | $\text{sec}^{-1}$             |
| $B^2_{3,2}$      | 0.014711  | 0.0149602             |                       | 0.014467             |                      | $\pm 0.002188$  | 1.50    | $\text{cm}^{-2}$              |
| $\lambda_{5,1}$  | 5436.598  | 5510.60               | 5463.24               | 5362.60              | 5409.96              | $\pm 74.0$      | 1.36    | $\text{sec}^{-1}$             |
| $B^2_{5,1}$      | 0.017171  | 0.0174476             |                       | 0.0168992            |                      | $\pm 0.000276$  | 1.61    | $\text{cm}^{-2}$              |
| $\lambda_{13,1}$ | 8689.778  | 8783.78               | 8711.44               | 8595.78              | 8668.12              | $\pm 94.0$      | 1.09    | $\text{sec}^{-1}$             |
| $B^2_{13,1}$     | 0.10606   | 0.10707               |                       | 0.10404              |                      | $\pm 0.00163$   | 1.91    | $\text{cm}^{-2}$              |
| $\lambda_0$      | 4759.765  | 4813.722              | 4764.832              | 4708.199             |                      | $\pm 54.0$      | 1.14    | $\text{sec}^{-1}$             |
| $D_0$            | 37084.23  | 37855.13              |                       | 36.87.06             | 37358.67             | $\pm 897$       | 2.42    | $\text{cm}^2 \text{sec}^{-1}$ |

TABLE IV

## CALCULATIONAL RESULTS

| Quantity         | Calculated By      | Value  | Maximum High Value | Maximum Low Value | Maximum Error | Maximum % Error | Units            |
|------------------|--------------------|--------|--------------------|-------------------|---------------|-----------------|------------------|
| $L^2$            | $D_o/\lambda_o$    | 7.79   | 8.04               | 7.52              | $\pm 0.27$    | 3.47            | $\text{cm}^2$    |
| L                | $\sqrt{L^2}$       | 2.79   | 2.84               | 2.74              | $\pm 0.05$    | 1.83            | cm               |
| $-B_o^2$         | $\lambda_o/D_o$    | 0.128  | 0.133              | 0.124             | $\pm 0.005$   | 3.91            | $\text{cm}^{-2}$ |
| $D_{th}$         | $D_o/220000$       | 0.169  | 0.172              | 0.164             | $\pm 0.005$   | 2.96            | cm               |
| $D_M$            | $D_o/248200$       | 0.149  | 0.153              | 0.146             | $\pm 0.005$   | 3.36            | cm               |
| $\Sigma_{ath}$   | $\lambda_o/220000$ | 0.0216 | 0.0219             | 0.0214            | $\pm 0.0003$  | 1.39            | $\text{cm}^{-1}$ |
| $\Sigma_{aM}$    | $\lambda_o/248200$ | 0.0192 | 0.0194             | 0.0190            | $\pm 0.0002$  | 1.05            | $\text{cm}^{-1}$ |
| $\lambda_{TRth}$ | $3D_o/220000$      | 0.506  | 0.516              | 0.494             | $\pm 0.01$    | 1.97            | cm               |
| $\lambda_{TRM}$  | $3D_o/248200$      | 0.448  | 0.458              | 0.437             | $\pm 0.011$   | 2.46            | cm               |
| $T_o$            | $1/\lambda_o$      | 210.1  | 212.4              | 207.7             | $\pm 2.4$     | 1.4             | $\mu\text{sec}$  |
| $T_{1,1}$        | $1/\lambda_{1,1}$  | 206.9  | 209.7              | 204.1             | $\pm 2.8$     | 1.35            | $\mu\text{sec}$  |
| $T_{3,1}$        | $1/\lambda_{3,1}$  | 197.8  | 200.6              | 195.1             | $\pm 2.8$     | 1.42            | $\mu\text{sec}$  |
| $T_{1,2}$        | $1/\lambda_{1,2}$  | 196.9  | 199.7              | 194.2             | $\pm 2.8$     | 1.42            | $\mu\text{sec}$  |
| $T_{3,2}$        | $1/\lambda_{3,2}$  | 188.7  | 191.3              | 186.1             | $\pm 2.6$     | 1.39            | $\mu\text{sec}$  |
| $T_{5,1}$        | $1/\lambda_{5,1}$  | 183.9  | 185.5              | 181.5             | $\pm 2.4$     | 1.31            | $\mu\text{sec}$  |
| $T_{13,1}$       | $1/\lambda_{13,1}$ | 115.1  | 116.3              | 113.8             | $\pm 1.3$     | 1.13            | $\mu\text{sec}$  |

emphasize the significance of a waiting time when applicable and the difficulties of obtaining a pure fundamental mode. The Maxwellian velocity ( $V_M = 2.482 \times 10^5$  cm/sec) (19) was used for the calculations of the parameters as well as the standard  $2.2 \times 10^{-5}$  cm/sec value.

Discrete modes were found which are rather close in value. If sufficient waiting time was not taken, an experimenter might indeed obtain a weighted average eigenvalue rather than a true eigenvalue (as 8). A waiting time of up to 50 fundamental decay periods as has been suggested (11) would more than suffice to eliminate or suppress higher harmonics.

In addition the largest term ( $2.97 \times 10^5 \text{ sec}^{-1}$ ) appeared to be an arbitrary amplitude and a decay constant existing above a given value for a particular position and starting channel. A fixed value was not confirmed but any computer value above  $2.85 \times 10^5 \text{ sec}^{-1}$  would suffice to produce iterations. Any value less or omission would reduce the iterations to shambles and the program would cease to iterate. The statistical accuracy and confidence in this term is small; however, the term would indicate a sort of "continuum" (as 5,22) or an arbitrary eigenvalue. An indication of an incapacity on the part of the computer analysis is more probable; however, the preceding conclusion is more interesting.

The equation  $\lambda_{1n} = \lambda_c + (n^2 - 1)D_0 B_c^2$  (11) for calculating higher modes was found to be well within statistical accuracy for two higher modes (1,2;3,2) using the two lower modes (1,1;3,1).

A symmetrical neutron density was obtained by locating the source in the medium being investigated. The perturbation of the density at the source due to the source tube appeared small. The drift tube was steel and apparently the scattering produced in the back direction compensated in part for the void. No dependence of results on detector position or waiting time for the harmonics reported and used was observed. The higher mode amplitudes were of the same order of magnitude as the fundamental. The computer analysis did indicate a reduction in amplitude and a subsequent loss in analysis sensitivity as a function of position for the two highest terms considered. The amplitude and decay constant of the highest term was a function of position and starting channel also.

With the source located inside the medium, the amount of shielding required is reduced considerably. At low duty cycles, it is even possible for the experimenter to reposition the detector without shutting off the neutron generator and thus maintain as closely as possible the previous source conditions.

Neither diffusion hardening or cooling was observed in the results. The latter was absent as a result of the size of the system. The absence of hardening of the spectrum may be due in part to the location of the source and source tube, and to the short times involved. The utilized data covered a maximum range of one to six mean thermal lifetimes. The source tube may have introduced sufficient cooling to offset any hardening.

Figures 12 and 13 are plots of  $\lambda_{ij}$  versus  $B_{ij}^2$  plots with figure 13 displaying the five lower points for clarity.

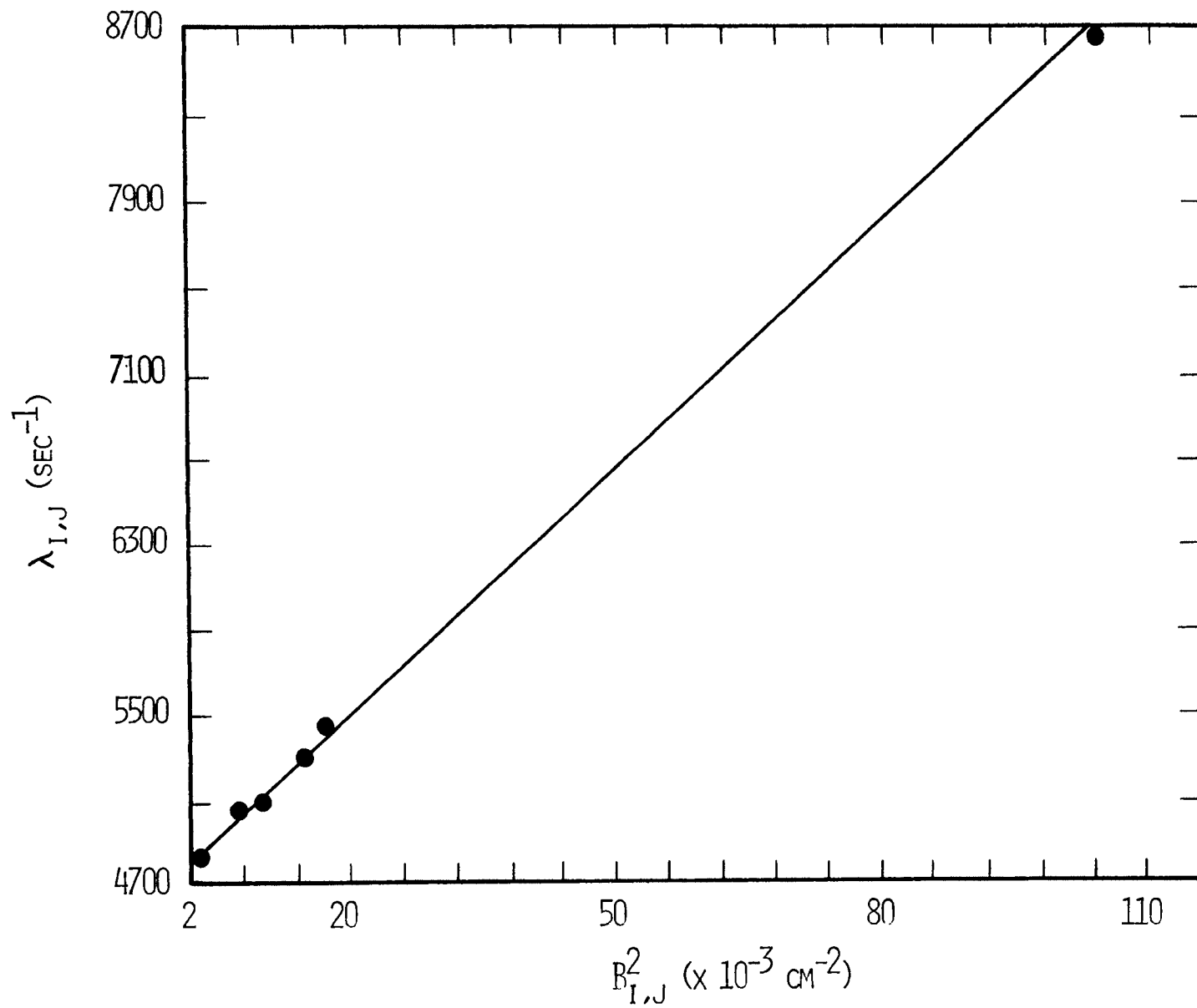


FIGURE 11, DECAY CONSTANTS VERSUS BUCKLING



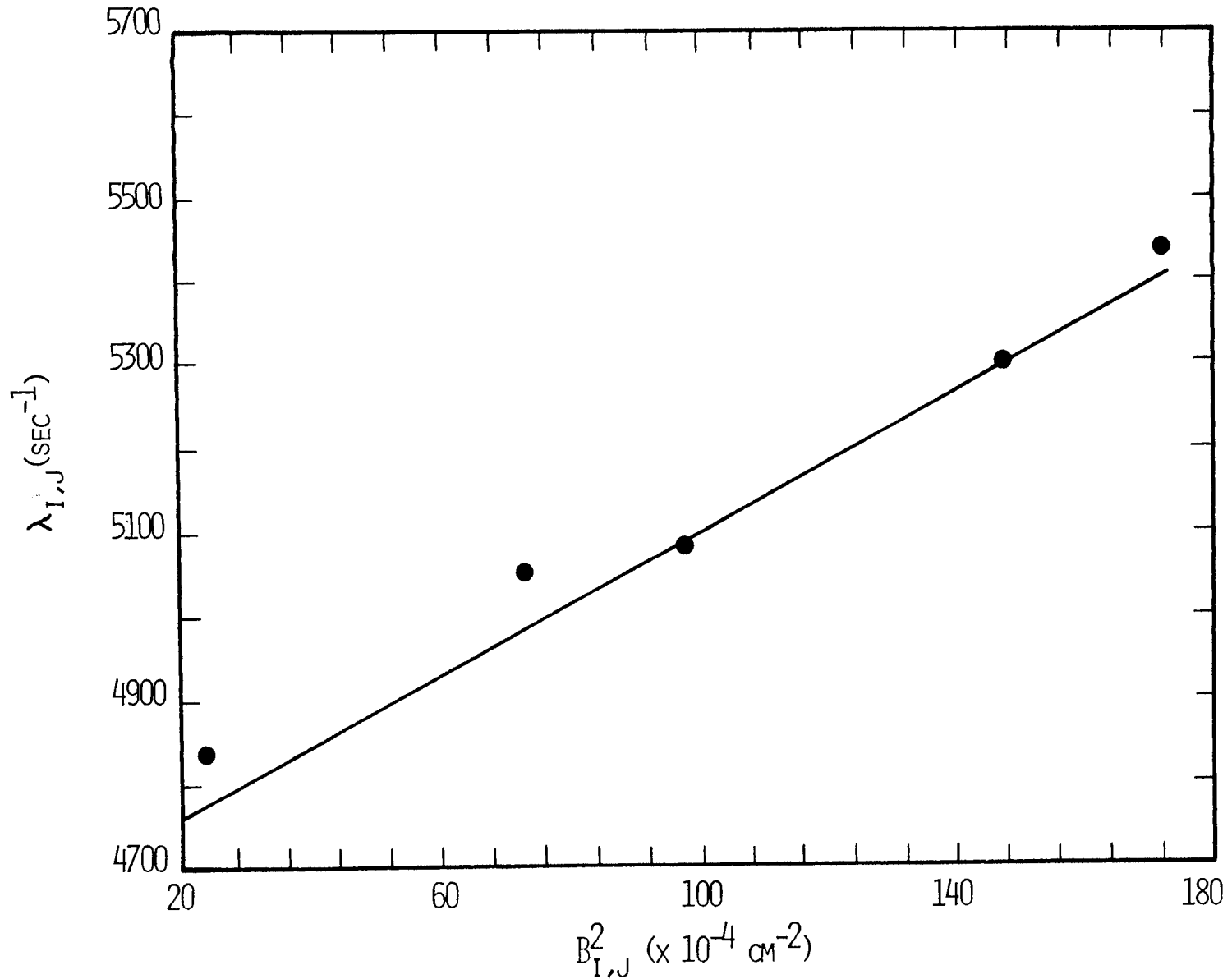


FIGURE 12, DECAY CONSTANTS VERSUS BUCKLING

## B. LABORATORY APPLICATION

By not being as sensitive to extrapolation distances, distance measurements, normalization calculations, accurate water heights, container perturbations, or not requiring an excess of electronic data acquisition equipment or an inordinate amount of time to acquire data, (14) this technique is ideally suited for student laboratories. By locating the source in the tank, the acquisition and statistics of the data is enhanced whereas the amount of shielding required is reduced. The large system is advantageous in that in conjunction with other equipment, it may also be used for other experiments such as Fermi age, diffusion length, spectra, etc. In one lab period, sufficient measurements and data could be taken in the axial direction to obtain the majority of reactor parameters. Given sufficient instructions and experience with the computer program, the data could be analyzed in a minimum amount of time. Thus one laboratory experiment would develop a significant number of reactor parameters.

## BIBLIOGRAPHY

1. Beckurts, K. H. Nuclear Instruments and Methods, 11, (1961), (1961), 144-168.
2. Beckurts, K. H. "A Review of Pulsed Neutron Experiments on Non-Multiplying Media," Pulsed Neutron Research, Volume I, International Atomic Energy Agency, Vienna (1965), 3-33.
3. Beckurts, K. H. and K. Wirtz. Neutron Physics. New York: Springer-Verlag Inc., 1964.
4. Cokinos, Dimitrios. "The Physics of Pulsed Neutrons," Advances in Nuclear Science and Technology. Edited by Paul Greebler and Ernest J. Henley, Volume 3, New York: Academic Press, 1966.
5. Corngold, Noel. Nuclear Science and Engineering, 19, (1964), 80-90.
6. Dambman, Dick. Kaman Nuclear, Personal Communication, 1969.
7. Foley, J. E. "Measurement of Thermal Neutron Decay Parameters in Water Using a Sinusoidal Source of Fast Neutrons," Doctoral Thesis, University of Arizona, 1969.
8. Ghatak, A. K. and H. C. Honeck. Nuclear Science and Engineering, 21, (1965), 227-239.
9. Kaman Nuclear, 1700 Garden of the Gods Road, Colorado Springs, Colorado 80907.
10. Keepin, G. R. LAMS-2215 (March, 1958).
11. Lopez, W. M. and J. R. Beyster. Nuclear Science and Engineering, 12, (1962), 190.
12. McWilliams, P. User's Guide - "Non-Linear Least Squares Program," 1965.
13. Menzel, J. H. R. E. Slovacek, and E. R. Gaerttner. Nuclear Science and Engineering, 42, 119-136 (1970).
14. Mesler, R. B., Harry G. O'Brien, and DeBow Freed. Nuclear Science and Engineering, 12, (1962), 79-81.
15. Moore, R. H. and R. K. Zeigler. "The Solution of the General Least Squares Problem with Special Reference to High-Speed Computers," LA-2367 (Physics and Mathematics TID-4500, 15th ed.), 1959.

16. Mosteller, Frederick, Robert E. K. Rourke, and George B. Thomas, Jr. Probability with Statistical Applications. Reading, Massachusetts: Addison Wesley Publishing Company, Inc., 1961.
17. Nasser, S. F. and G. Murphy. Nuclear Science and Engineering, 35, (1969), 70.
18. Nelkin, Mark. Nuclear Science and Engineering, 7, (1960), 210-216.
19. Proceedings of the Symposium on Pulsed Neutron Research, IAEA, Karlsruhe, Volumes I and II, May 1965.
20. Reactor Physics Constants, ANL-5800, USAEC, 1963.
21. Scott, F. R., D. B. Thomson, and W. Wright. Physics Review, 95, (1954), 582.
22. Shapiro, C. and N. Corngold. Physical Review, 137, 6A, A1686, (1965).
23. Sjostrand, N. G. Nukleonik, Band 1, Heft 3, August 1958, Page 89.
24. Snedecor, George W. and Silliam G. Cochran. Statistical Methods. 6th Edition. Ames, Iowa: Iowa State University Press, 1967.
25. Van Dardel, G. F. Trans. Royal Institute of Technology, Stockholm, 75, 1, (1954).
26. Von Dardel, G. and N. G. Sjostrand. Physical Review, Vol. 96, (1954), 1245.

## VITA

Harold David Hollis was born October 25, 1932 in Clinton, Missouri to Elsie and William Hollis.

After graduating from Clinton High School, he served two years with the United States Army Artillery and was honorably discharged with the rank Sergeant First Class.

1958 was a turning point in his life when he decided to get a college education and was married. He began his first year of college in Kansas City, Missouri at Rockhurst College. Then he transferred to Central Missouri State College, where he graduated in 1962 with a B.S. in Physics and a B.A. in Mathematics.

In 1964, he obtained his M.S. in Physics at the University of Missouri-Columbia after which he accepted a position with Central Missouri State College teaching physics.

During the summer of 1966, he attended the University of Missouri-Rolla on a NSF Summer Institute. At this time he met Dr. William H. Webb and Dr. D. R. Edwards who encouraged him to apply for financial assistance and return to school for a Ph.D.

Following this advice, he received an AEC Traineeship from the University of Missouri-Rolla, changed his major, and began studying in the field of nuclear engineering. He subsequently received three AEC special fellowships to finish his graduate work.

He is a member of Sigma Zeta, Sigma Xi, a student member of American Nuclear Society and American Association of Physics Teachers.

APPENDIX I  
STATISTICS

The computer program (12,14) used to calculate the amplitudes and decay constants also calculated certain statistical measures of the fit. The weighted variances [Variance =  $\sum_{N=1}^N W_i (Y - Y_{\text{calculated}})_i^2 / (N - (\text{Number of Parameters}))$ ] were found to be proportional to position due to the significantly higher counts recorded at positions nearer the source. The unweighted sum of squares of the deviations ran from  $10^3$  for points close to the source out to about  $10^1$ . The standard deviation of the Kth parameter was never greater than .5%. The fitted function compared to the input data was about one unit in the second to the third place. For all data sets, the standard deviation of the predicted mean varied between  $10^{-2}$  to one as the minimum and maximum found on any data set. Tables V and VI list the diverse statistical parameters calculated from the distributions of the decay constants.

Two different programs were utilized to calculate the fit of the decay constants to the bucklings. Both gave the same values down to the decimal point. One program calculated the degree of the polynomial that gave the best fit as well as other statistical parameters. A first degree polynomial gave the best fit for the six points as well as for combinations of lesser numbers of points. The average per cent error of the points was 0.38%. The variance, using five degrees of freedom, was 992.317. This would give a standard deviation for the decay constants of 31.6 which is closer to the standard deviation values found from the distributions than the  $\sqrt{\lambda}$  values assumed for the errors.

TABLE V  
STATISTICAL RESULTS

| $\frac{\sum \lambda_i}{N}$<br>Average Value<br>Decay<br>Constant | N<br>No. In<br>Sampling | Indices<br>m,n        | $\sqrt{\frac{\sum (\lambda_i)^2}{N}}$<br>Root Mean<br>Square | $\frac{\sum (\lambda_i - \lambda_{ave})}{N-1}$<br>Mean<br>Deviation | $\sqrt{\frac{\sum (\lambda_i - \lambda_{ave})^2}{N-1}}$<br>Standard<br>Deviation | $\frac{\sum (\lambda_i - \lambda_{ave})^2}{N-1}$<br>Variance | $\sum (\lambda_i - \lambda_{ave})$<br>Sum of<br>Deviations |
|--|-------------------------|-----------------------|--|---|--|--|--|
| 297345.060   | 51                      | (?,?)no<br>confidence | 298052.750   | 16688.60  | 20758.30   | 4.309 x 10 <sup>8</sup>                                      | -2.063   |
| 15087.691  | 51                      | (?,?)no<br>confidence | 15095.957  | 58.06   | 91.86  | 8439.18  | -0.082   |
| 8689.778   | 51                      | (13,1)                | 8689.778   | 14.20   | 21.66  | 469.26   | -1.016   |
| 5436.598   | 51                      | (5,1)                 | 5436.652   | 21.58   | 26.64  | 709.93   | -1.035   |
| 5300.004   | 13                      | (3,2)                 | 5300.008   | 6.74  | 8.77   | 76.9   | -0.027   |
| 5078.363   | 13                      | (1,2)                 | 5078.363   | 3.37  | 4.34   | 18.81  | -0.059   |
| 5055.117   | 13                      | (3,1)                 | 5055.125   | 6.83  | 8.05   | 64.83  | -0.059   |
| 4834.391   | 51                      | (1,1)                 | 4834.469   | 21.82   | 28.91  | 835.73   | -0.910   |

TABLE VI  
STATISTICAL RESULTS

| Average Value<br>Decay<br>Constant | <u>Mean Deviation</u><br>Standard Deviation | Fraction of Times<br>Deviation > Std. Dev. | Fraction of Times<br>Dev. > 2σ | Median   | Numbers<br>Within<br>-σ to +σ |
|------------------------------------|---|--|--------------------------------|----------|-------------------------------|
| 297345.060                         | 0.80  | $\frac{16}{51} = 0.314$                    | $\frac{2}{51} = 0.0393$        | ----     | 32                            |
| 15087.691                          | 0.63  | $\frac{8}{51} = 0.157$                     | $\frac{1}{51} = 0.0195$        | ----     | 40                            |
| 8689.778                           | 0.65  | $\frac{11}{51} = 0.216$                    | $\frac{6}{51} = 0.118$         | 8684.169 | 36                            |
| 5436.598                           | 0.81  | $\frac{15}{51} = 0.288$                    | $\frac{2}{51} = 0.0393$        | 5429.626 | 32                            |
| 5300.004                           | 0.77  | $\frac{3}{13} = 0.23$                      | $\frac{1}{13} = 0.077$         | 5302.401 | 10                            |
| 5078.363                           | 0.78  | $\frac{3}{13} = 0.23$                      | $\frac{1}{13} = 0.077$         | 5078.605 | 12                            |
| 5055.117                           | 0.85  | $\frac{4}{13} = 0.308$                     | $\frac{0}{13} = 0.0$           | 5055.738 | 13                            |
| 4834.391                           | 0.75  | $\frac{10}{51} = 0.195$                    | $\frac{2}{51} = 0.0393$        | 4832.784 | 37                            |



The errors associated with the decay constants were assumed to be the square root of the value since the distributions were slightly sharper than a Poisson (15,23). This would give a maximum error since all the values fell within plus or minus this value. Throughout the error analysis, the maximum errors were assumed in obtaining all quantities. This then gives an upper bound for errors on all values found or calculated. These maximum and minimum values were input to the program to find the maximum and minimum values of  $\lambda_0$  and  $D_0$  as well as to attempt to find minimum errors. A large variety of combinations of the maximum deviations of the bucklings, considering a half centimeter variation in the radius and a centimeter variation in height, and the maximum deviations of the decay constants were least square fitted. The results are given in Tables III and IV.

In some cases no minimum errors were found or the values were so close that no value was listed. Variations of height and radius up to one inch were then fitted, assuming the decay constants were correct. These results fell within the maximum errors found. The assumption above of the worst possible world does not give exceedingly large errors for the parameters calculated. These errors are greater than normally calculated errors.

No analysis was attempted on the amplitudes since computer outputs suggested a certain lack of sensitivity inherent to the amplitudes in points from 30 centimeters on out in any direction in the system. Regardless of the method of normalization, magnitude values

could be varied after convergence with iteration changes occurring very slowly in points removed from the source. The crossings and maxima and minima locations were considered in the identification and description.

Table VII enumerates a set of data corrected by subtracting cadmium covered detector data and background. The first channel listed is channel thirteen. These data were taken at a radial distance of sixteen inches with a repetition rate of 25 cycles/sec with a 50  $\mu$ sec pulse width. The channel immediately following the last channel given in the table contained thirteen counts and consequently it and all succeeding channels were eliminated.

TABLE VII  
CORRECTED DATA SET

| <u>Time ( sec)</u> | <u>Channel Count</u> |
|--------------------|----------------------|
| 0.3313E-03         | 5661.77              |
| 0.3563E-03         | 4762.45              |
| 0.3813E-03         | 4269.70              |
| 0.4063E-03         | 3824.68              |
| 0.4313E-03         | 3223.15              |
| 0.4563E-03         | 2801.47              |
| 0.4813E-03         | 2710.27              |
| 0.4563E-03         | 2801.47              |
| 0.4813E-03         | 2710.27              |
| 0.5063E-03         | 2267.23              |
| 0.5313E-03         | 1986.27              |
| 0.5563E-03         | 2208.84              |
| 0.5813E-03         | 1544.54              |
| 0.6063E-03         | 1342.54              |
| 0.6313E-03         | 1252.04              |
| 0.6563E-03         | 1121.48              |
| 0.6813E-03         | 867.54               |
| 0.7063E-03         | 821.42               |
| 0.7313E-03         | 630.69               |
| 0.7563E-03         | 562.87               |
| 0.7813E-03         | 565.74               |
| 0.8063E-03         | 506.29               |
| 0.8313E-03         | 455.13               |
| 0.8563E-03         | 394.05               |
| 0.8813E-03         | 430.30               |
| 0.9063E-03         | 271.36               |
| 0.9313E-03         | 270.47               |
| 0.9563E-03         | 296.85               |
| 0.9813E-03         | 178.97               |
| 0.1006E-02         | 177.78               |
| 0.1031E-02         | 136.87               |
| 0.1056E-02         | 100.15               |
| 0.1081E-02         | 119.72               |
| 0.1106E-02         | 113.30               |
| 0.1131E-02         | 94.04                |
| 0.1156E-02         | 83.76                |
| 0.1181E-02         | 70.59                |
| 0.1206E-02         | 74.62                |
| 0.1231E-02         | 78.68                |
| 0.1256E-02         | 41.84                |
| 0.1281E-02         | 87.86                |

APPENDIX II  
RECOMMENDATIONS

For data acquisition, it would be recommended to use a higher cycling rate of about thirty-five or forty cycles per second. Thus more data would be taken in an equivalent time. It appears redundant to analyze any data except that taken in the vertical plane containing the source tube. All necessary information may be obtained in this plane and flux perturbations caused by the source tube might be introduced in other directions. Data normalization would be improved by utilizing either a cadmium covered detector or a fast neutron detector to normalize each run to a given number of counts, i.e., 60,000. This normalizing detector should be located on the tank wall in the source plane on the extremity of the radial line of the source tube. This detector connected to a single channel scaler was used during final data runs and improved statistics at data points far removed from the source. As the target foil becomes "used," the normalization by any other method will become more difficult. With a fast neutron detector, the location could either be the one mentioned previously or be at the point where the drift tube enters the tank. The difficulty with this location would be the neutrons created during the "off" of the generator; however, the total count could be increased accordingly.

The height of the water was approximately twice the radius of the tank. If at all possible, any additional work should change the

height to as large a difference as possible from a simple multiple of the radius. The pulse of source neutrons would not then arrive at the closest boundary faces at virtually the same time. Any scattering effects and room return neutrons would be further reduced in time.

For data analysis, the amplitudes should be initially input at a positive  $5 \times 10^4$  value. The decay constant guesses may be obtained from graphing various channel portions of any of the data sets. As iterations proceed, any terms of the expansion that have amplitudes that are consistently low ( $10^2$  or less) over all space may be eliminated without hesitation. Any term that is very slow to converge or appears inconsistent should be duplicated in the expansion. This is an empirical observation as a result of the experience with the decay constant of value 5200. Introducing duplicate terms will either cause convergence or an additional term should be introduced. Persistence and patience are required if large amounts of data are to be analyzed. Data points need not be too close together to obtain an adequate mapping of lower decay mode amplitudes.

The convergence of the data should also be more restrictive on the amplitudes. Additional computer time to improve amplitudes would not effect decay constant values but would assist in index identification. Some information might be gained by computer analysis of the fast data taken with the cadmium covered detector or a fast neutron detector.

A known code was used in this instance; however, the program was general and not specific for this situation. The development of a

computer program with acceleration techniques would be advantageous.

It would also be of interest to repeat a similar experiment with fuel in the system. Basic reactor parameters could be measured under more advantageous conditions of symmetry. Reactivity, lifetimes, absorption cross sections, and diffusion areas could be obtained. Homogeneity and change of parameters with loadings could be studied. Other parameters could be considered and measured by varying the loadings, voiding the centers of fuel, the implacement of black or grey rods in either a water or a water fuel system, the introduction of other reactor materials, or by the construction and insertion of specialized energy detectors of unusual shape.

The "energy trapping" or delayed decay phenomena should be further investigated to determine causes, cross sections or channels, or the related times required to establish a given asymptotic flux. The observed anomalous decay may be due to one of four causes. Equipment, group velocity, 14 Mev source neutron decay and established flux decay, or finite time required to establish an asymptotic flux at a given position may be responsible. Many questions related to this problem could be resolved by performing the same experimental steps only with graphite or another material as the moderator.

APPENDIX III  
BUCKLINGS AND AMPLITUDES

For the buckling calculations, the height of the tank was considered as the extrapolated height of the tank of water. The void at the center was then corrected for as well as the aluminum fuel plates at the bottom of the tank, the tube walls, and the tank walls by

$$d' = d \frac{\lambda_{TR}(H_2O)}{\lambda_{TR}(\text{Medium})}$$

where  $\lambda_{TR}(\text{Aluminum}) = 10.3 \text{ cm}$

$$\lambda_{TR}(\text{Steel}) = .875 \text{ cm}$$

$$\lambda_{TR}(H_2O) = .434 \text{ cm}$$

$$d(\text{extrapolation}) = .71 \lambda_{TR}$$

The values were calculated from information in ANL-5800 (20) and as a result the height was 126.44 cm and the radius was 57.7 cm. In addition, the bucklings were calculated for a possible error of  $\pm 0.5$  cm in radius and the height  $\pm 1.0$  cm. These extremes were utilized in the calculation of maximums and minimums of the parameters. As a result of these findings, most of the above calculations could be eliminated in a student laboratory on a large system. The height and radius were then input to a computer program to calculate  $B^2$  from:

$$B_{ij}^2 = (i\pi/H)^2 + (\alpha(j)/R)^2$$

where the  $\alpha(j)$ 's are the zeroes of  $J_0$ .

The equation  $A_{ij} = (\cos \frac{i\pi z}{H} J_0(\alpha(j)r/R))/\rho$  was used to calculate theoretical amplitudes to identify the associated decay constants

with the  $i, j$  bucklings using the sign changes rather than absolute magnitudes, where  $\rho^2 = (r^2 + z^2)$ . Figures 13 and 14 are plots of the total amplitude versus position for the axial and radial directions for various times after the initialization of the source pulse. Both plots display a  $1/\rho^2$  shape (11) as a result of the attenuation in the medium of the point source. The manufacturer (9) suggests that the source appears as a point source at a distance of eleven centimeters from the target. No data sets were completely analyzed at any distance closer than five inches in the medium.

The amplitudes and the total neutron density in the radial source plane were symmetric in the three directions considered. There was a slight deviation from expected magnitude near the source tube; however, this was minimized by not taking data at positions in the close proximity of the tube (figures 16, 20, 21, 22, 23). Figures 15 through 24 are plots of theoretical amplitudes modified by  $1/\rho^2$  and experimental data points for the amplitudes of interest. The data displayed for the radial direction was taken along the diameter of the source tube.

Some general relationships are readily apparent. The majority of the plots appear shifted up in magnitude and away or out in position. This appears more pronounced in figure 23. The points relatively close to the source (11 cm) are scattered in magnitude as in figure 20. The negative portions are either suppressed or "raised" as in figure 18 for the majority of the plots. Figure 21 was the only plot where the converse was true. For the lowest mode, all



plots displayed a small "hump" about half way between the source and the boundary. This position would roughly correspond to the optimum position at the center that most experimenters utilize. The amplitude plots would indicate a reinforced amplitude or constructive interference at the region of the midpoint. The plots in general, especially for the lowest and the highest modes, fit the  $(\cos \frac{j\pi z}{H} J_0(\alpha(j)r/R))/\rho^2$  plots better than any other function. Except for figures 21, 23, 24, all other plots or amplitude identification was straight forward and did not require interpretation.

Figures 15 through 18 are the four modes in the axial direction. Figure 16 is the lowest mode ( $I=1$ ). A deviation from the theoretical shape may be seen at points close to the distance at which the source appears as a point source and a smaller hump about halfway between the source and the boundary. Figure 16, the second mode ( $I=3$ ), displays these deviations again. The magnitude of the data points beyond midpoint of the system have a probable error of  $\pm 10\%$ . Figures 17 and 18 demonstrate the overall increase in magnitude and shift of the sign changes away from the source.

The radial amplitudes (figures 19, 20, 21) display the scattering of amplitudes near the source with figure 20 showing the hump near midpoint. In figure 21, the negative amplitude is greater than the solid line indicative of the expected values. Figures 22, 23, and 24 of the  $45^\circ$  direction display the characteristics of the other plots. The fundamental (figure 22) has the scatter in magnitude near

the source and the added magnitude at the midpoint. Figure 23 displays the extreme plot where the amplitudes are increased in magnitude and the sign change positions are shifted away from the source. In Figure 24, the positive amplitudes are enhanced while the negative amplitudes are suppressed.

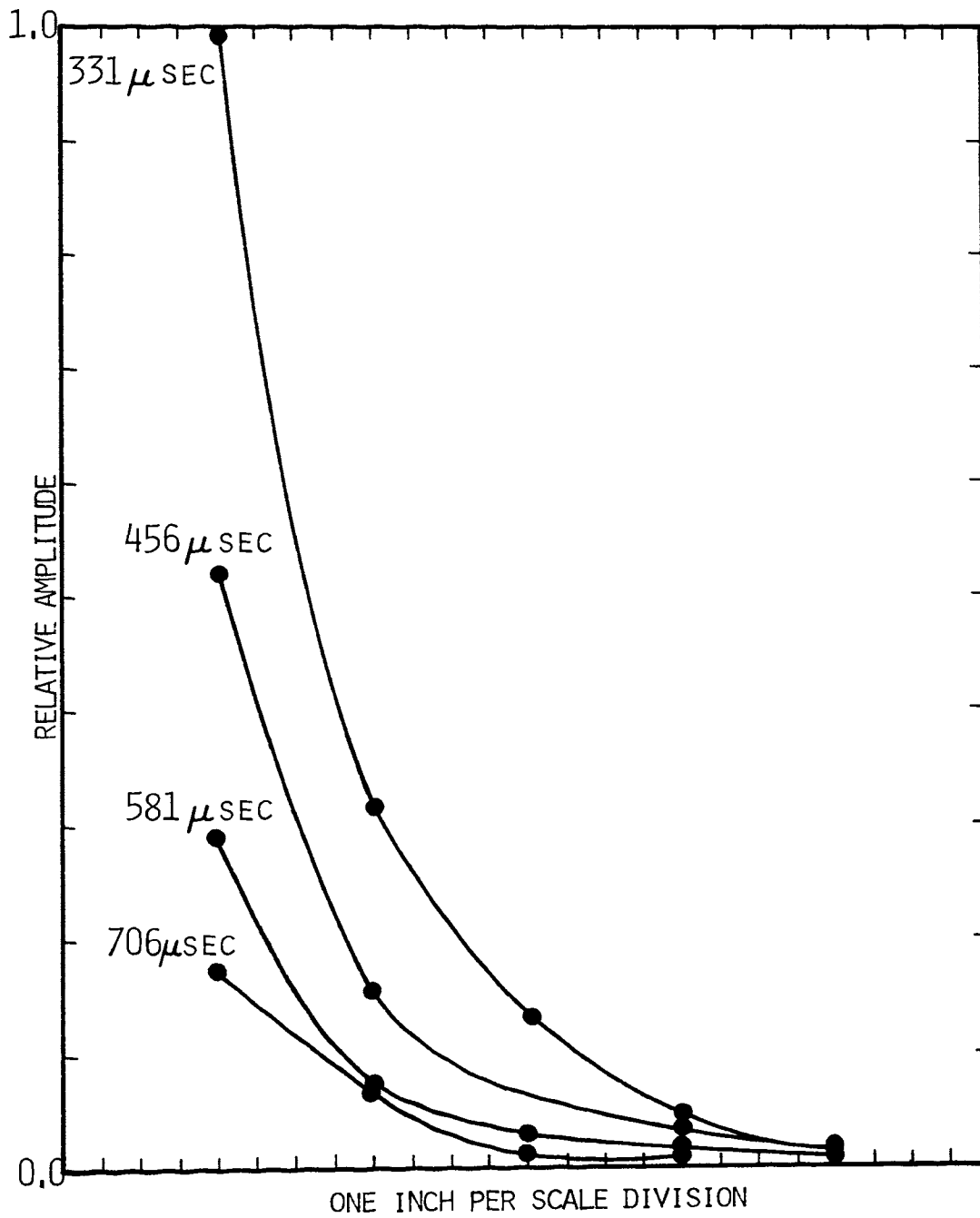


FIGURE 13. TOTAL RELATIVE AMPLITUDE VERSUS AXIAL POSITION

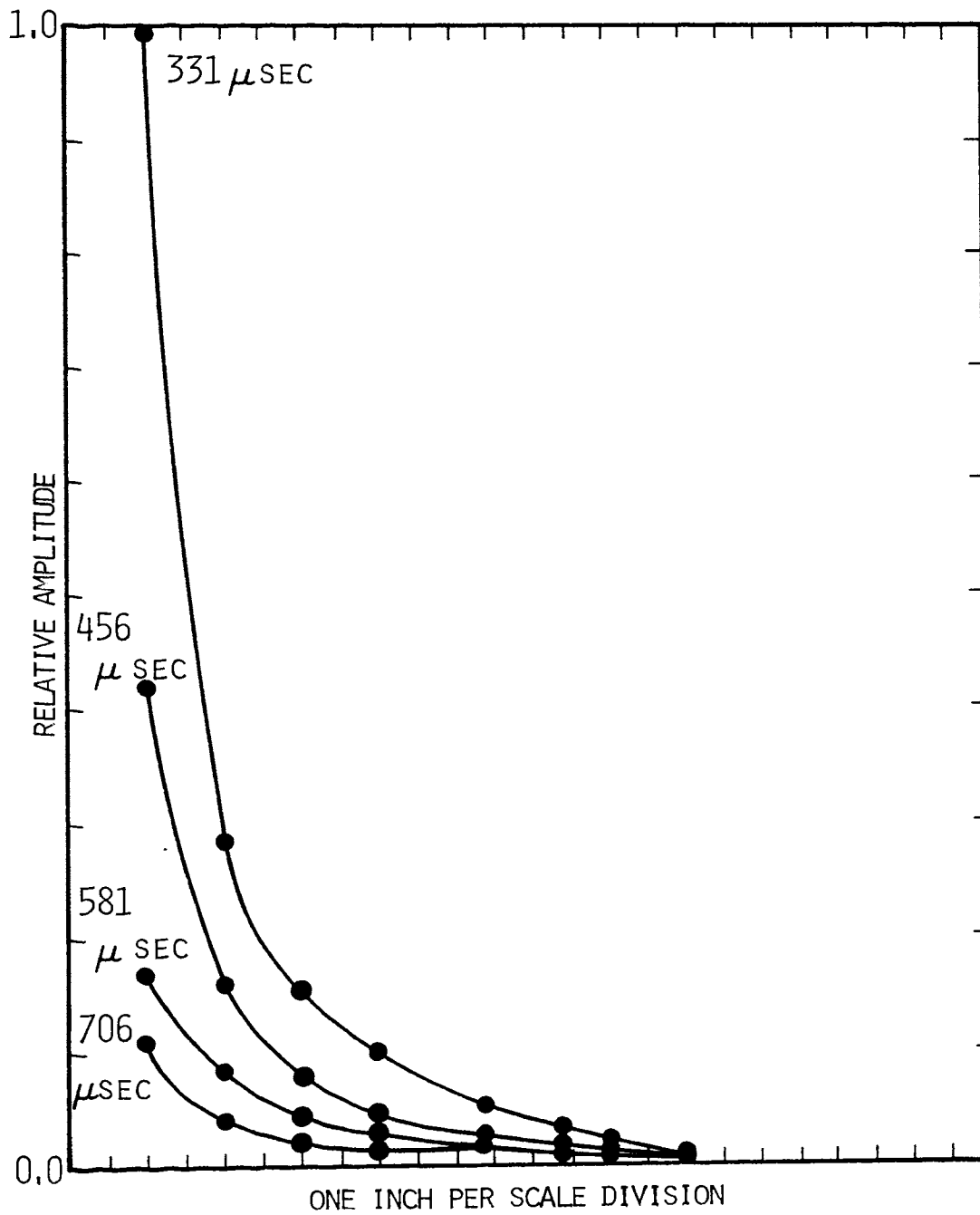
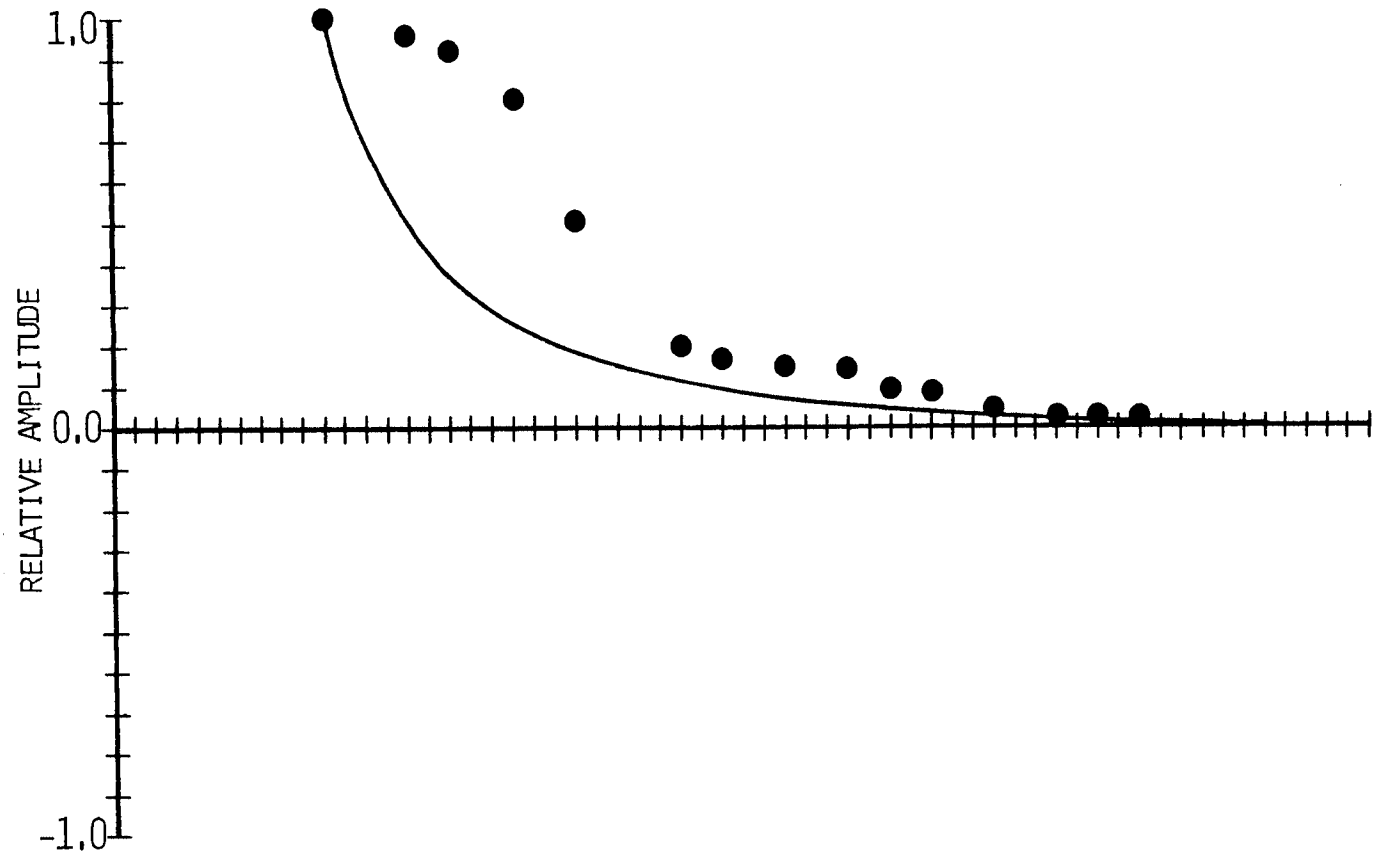
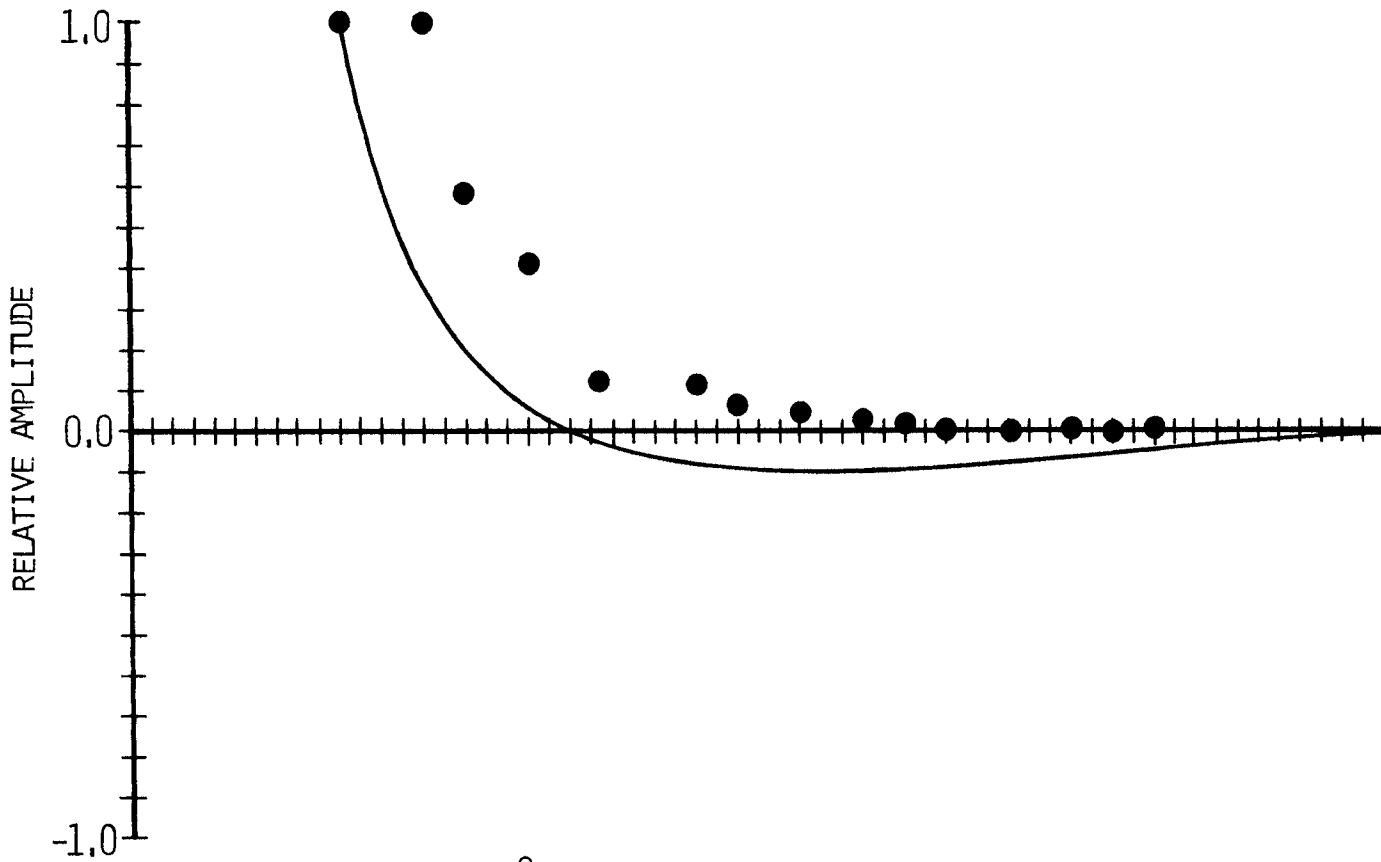


FIGURE 14. TOTAL RELATIVE AMPLITUDE VERSUS RADIAL POSITION



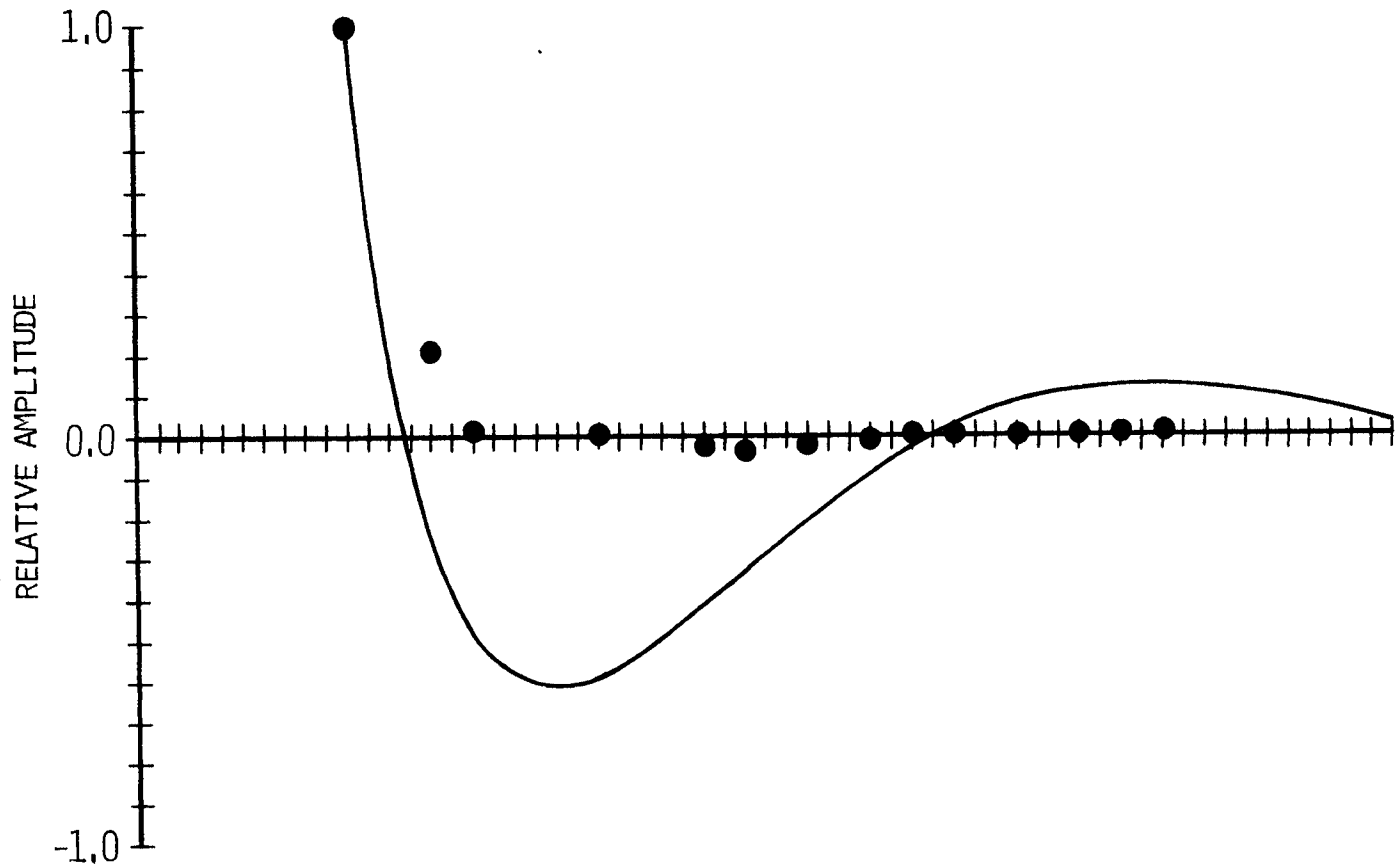
ONE CENTIMETER PER SCALE DIVISION

FIGURE 15. RELATIVE AMPLITUDE VERSUS AXIAL DISTANCE FOR I=1



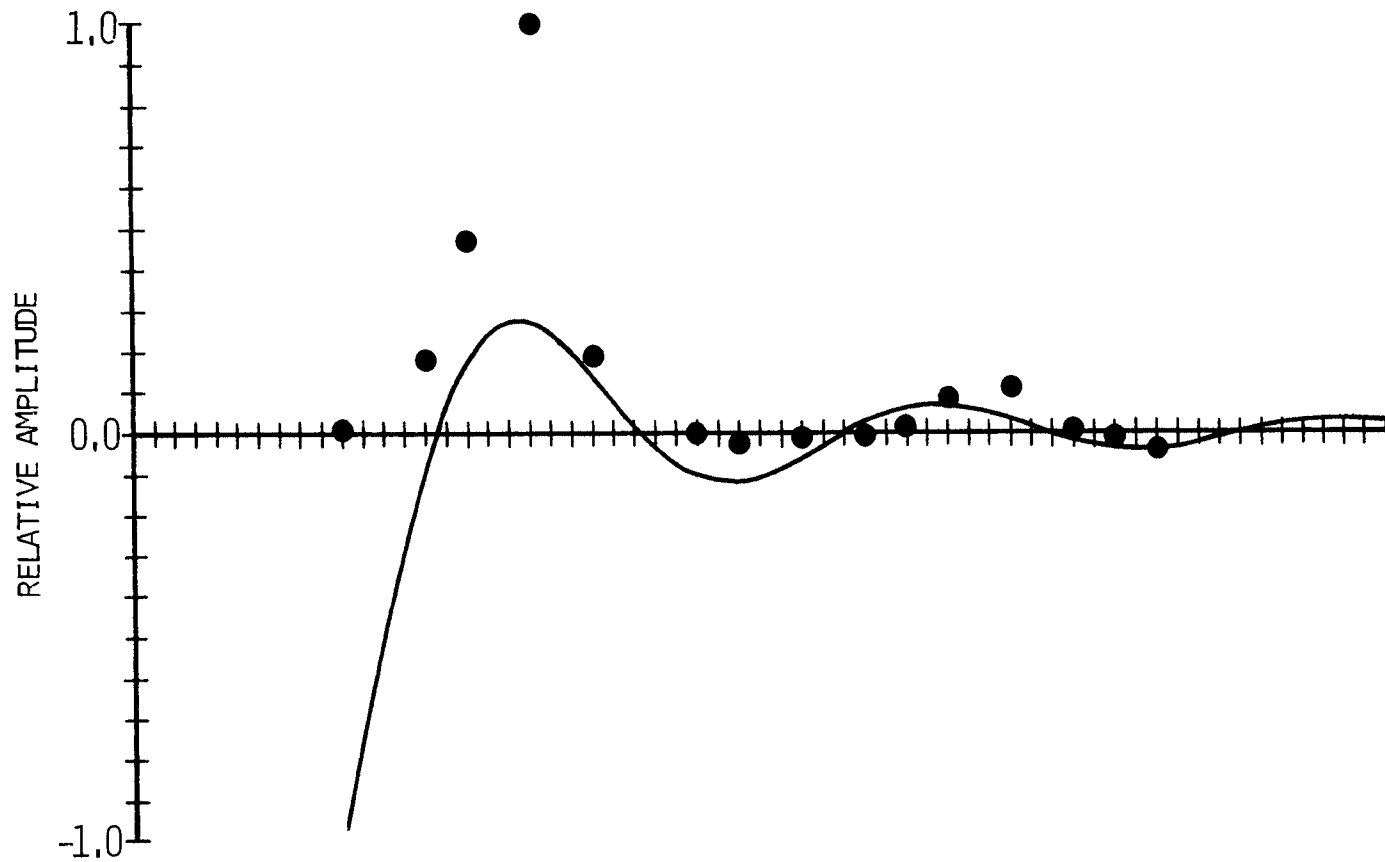
ONE CENTIMETER PER SCALE DIVISION

FIGURE 16. RELATIVE AMPLITUDE VERSUS AXIAL DISTANCE FOR  $I=3$



ONE CENTIMETER PER SCALE DIVISION

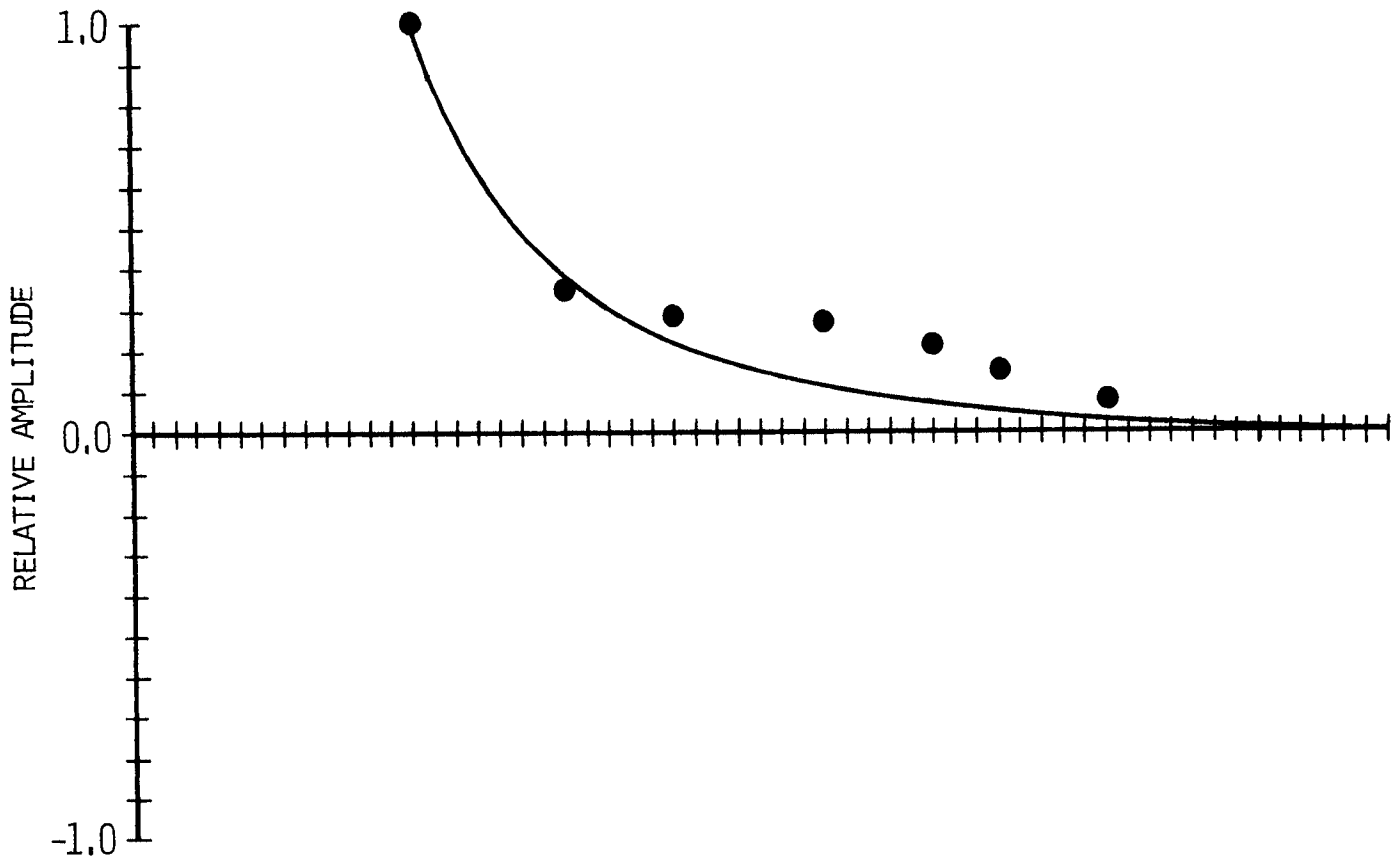
FIGURE 17. RELATIVE AMPLITUDE VERSUS AXIAL DISTANCE FOR I=5



ONE CENTIMETER PER SCALE DIVISION

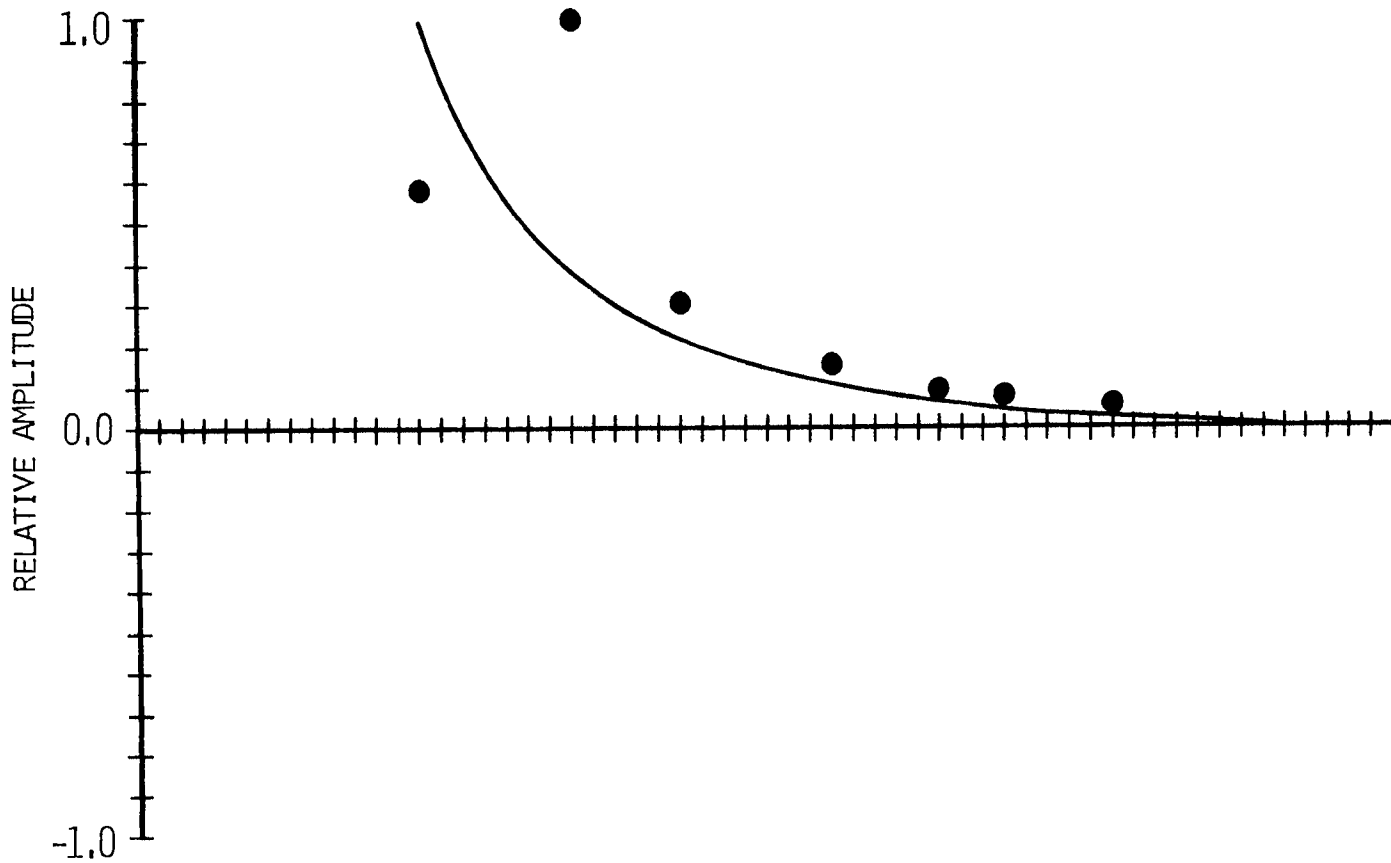
FIGURE 18. RELATIVE AMPLITUDE VERSUS AXIAL DISTANCE FOR  $I=13$





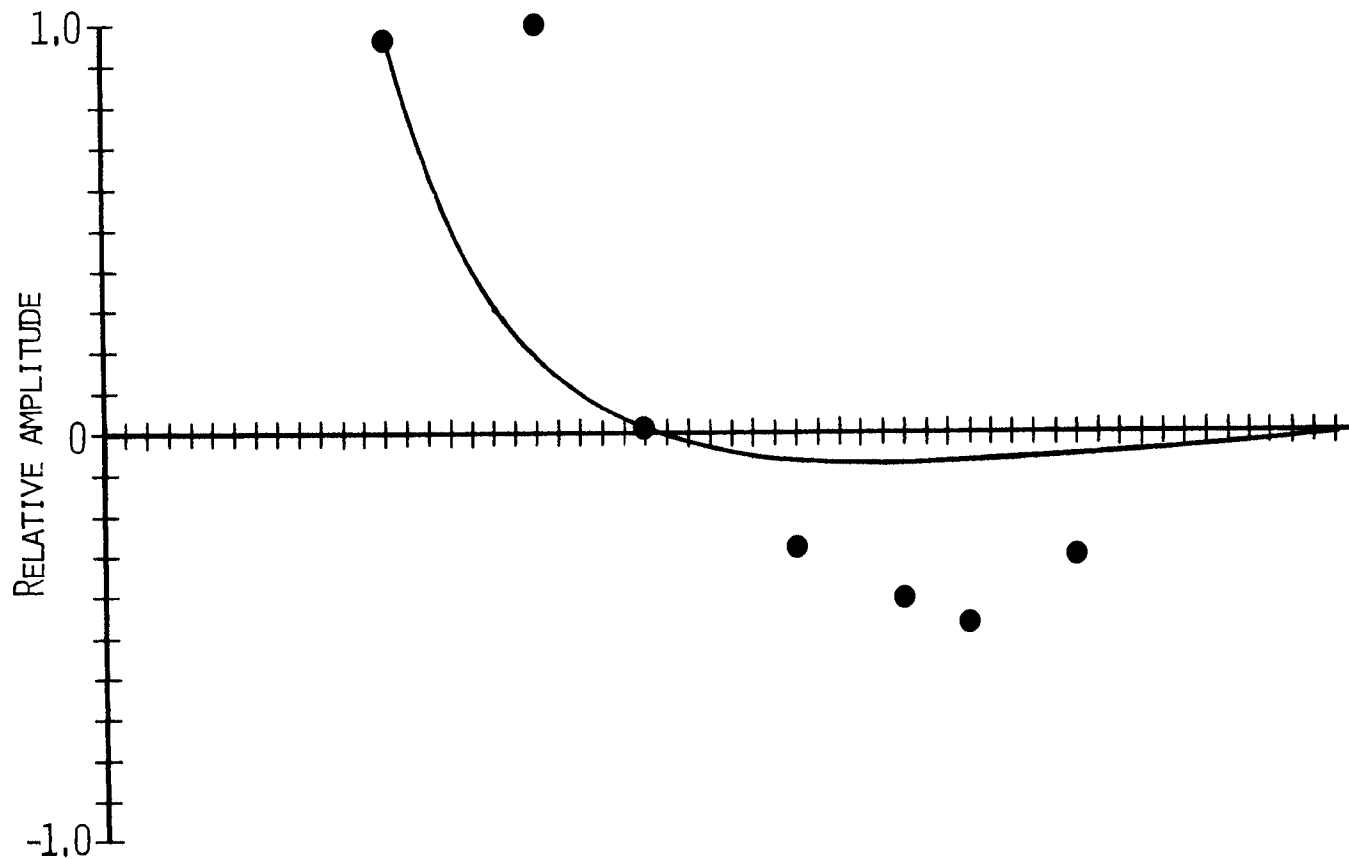
ONE CENTIMETER PER SCALE DIVISION

FIGURE 19, RELATIVE AMPLITUDE VERSUS RADIAL DISTANCE FOR J=1



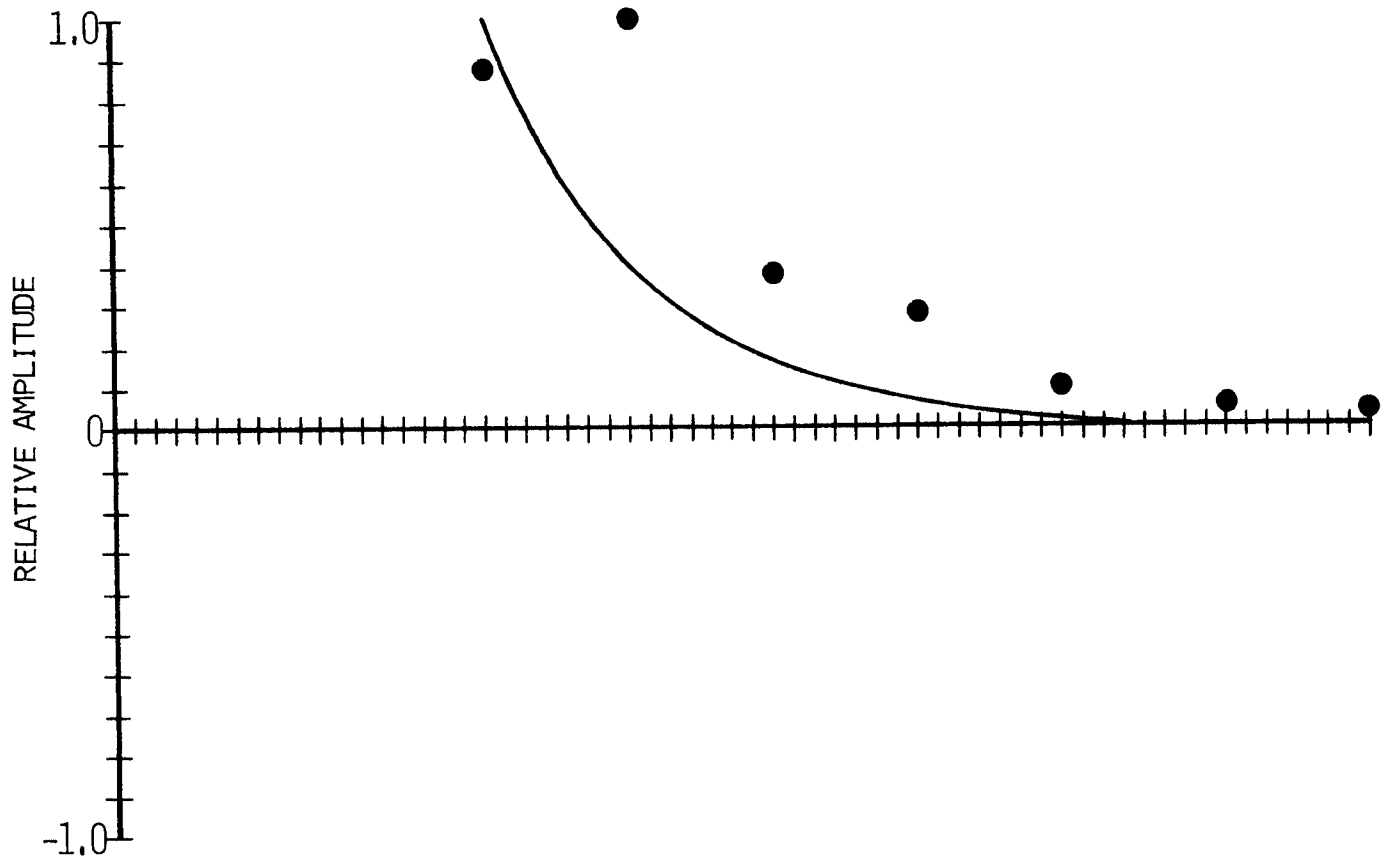
ONE CENTIMETER PER SCALE DIVISION

FIGURE 20. RELATIVE AMPLITUDE VERSUS RADIAL DISTANCE FOR HIGHER MODES WITH  $J=1$



ONE CENTIMETER PER SCALE DIVISION

FIGURE 21. RELATIVE AMPLITUDE VERSUS RADIAL DISTANCE FOR  $J=2$



ONE CENTIMETER PER SCALE DIVISION

FIGURE 22. RELATIVE AMPLITUDE VERSUS DISTANCE ALONG  $45^\circ$  DIRECTION FOR  $I=1, J=1$

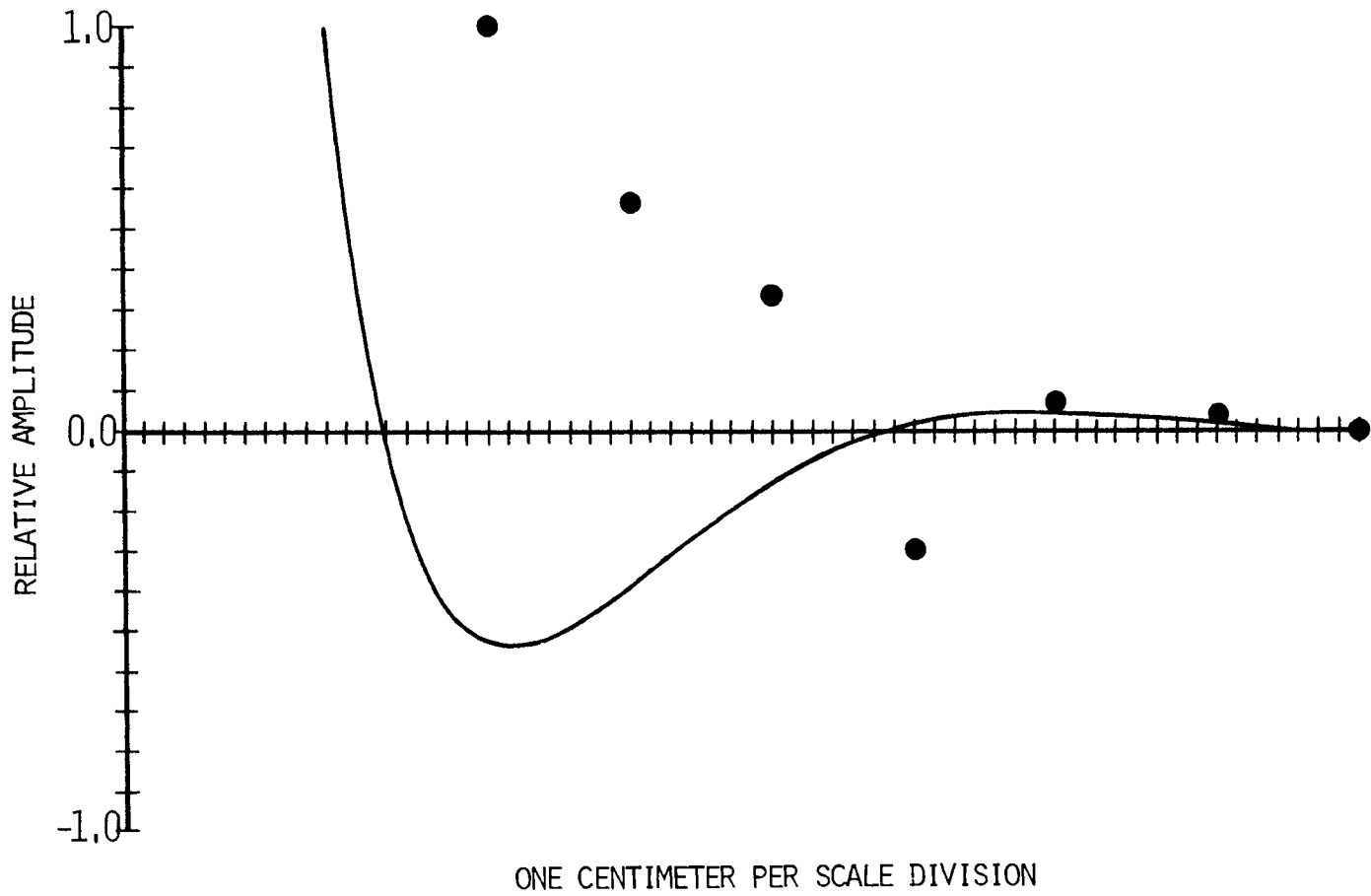
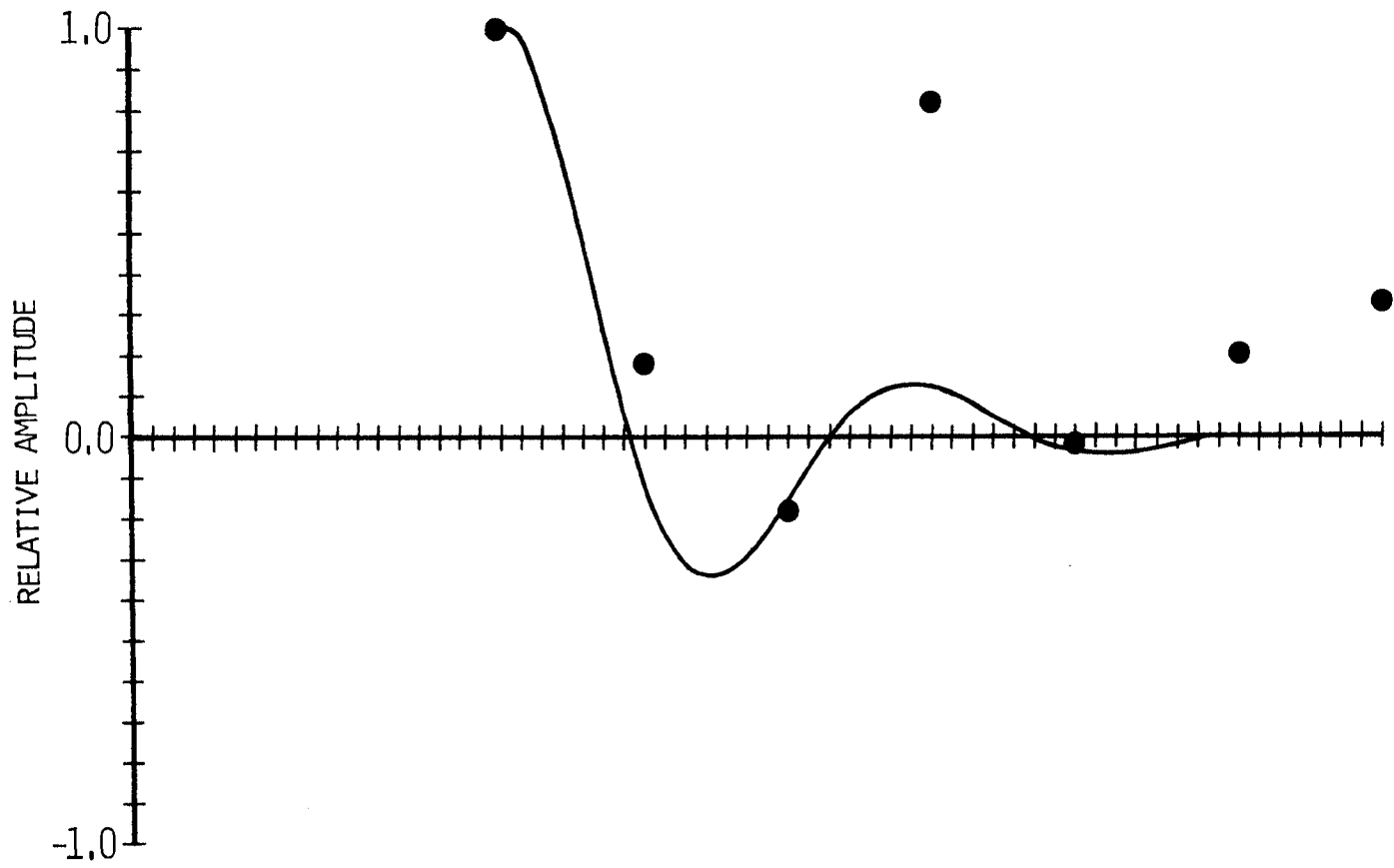


FIGURE 23. RELATIVE AMPLITUDE VERSUS DISTANCE ALONG 45° DIRECTION FOR I=5, J=1



ONE CENTIMETER PER SCALE DIVISION

FIGURE 24. RELATIVE AMPLITUDE VERSUS DISTANCE ALONG 45° DIRECTION FOR I=13, J=1